OPTICAL STUDIES OF COLLAGEN CROSSLINKING, ANGIOGENESIS AND MATRIX METALLOPROTEINASES

by

William Rudy Brands

A Report Submitted to the Faculty of the

GRADUATE INTERDISCIPLINARY PROGRAM IN

BIOMEDICAL ENGINEERING

In Partial Fulfillment of the Requirements

For the Degree of

MASTER OF SCIENCE

WITH A MAJOR IN BIOMEDICAL ENGINEERING

In the Graduate College

THE UNIVERSITY OF ARIZONA

2007

Abstract

A blood circulatory system (vasculature) is an essential structure in multicellular organisms for distribution of oxygen and nutrients. Angiogenesis, the formation and growth of new blood vessel sprouts from existing vessels, is the process by which additional vascular elements are formed from an initial vascular structure. During angiogenesis, endothelial cells are stimulated to exhibit migratory and proliferative phenotypes, leading to the formation of new vessel sprouts. Sprouting endothelial cells degrade their basement membrane by production of matrix metalloproteinases (MMPs). In an effort to understand the role of certain MMPs during the sprouting process, the rat fat microvessel fragment 3D model of angiogenesis was used to immunostain for the presence of MMP-2, MMP-9 and MT1-MMP at several stages of the sprouting process.

Background

A blood circulatory system (vasculature) is an essential structure in multicellular organisms for distribution of oxygen and nutrients, thereby overcoming the limits of oxygen diffusion. Angiogenesis, the formation and growth of new blood vessel sprouts from existing vessels, is the process by which additional vascular elements are formed from an initial vascular plexus. During angiogenesis, previously quiescent endothelial cells are stimulated to exhibit migratory and proliferative phenotypes, leading to the formation of new vessel sprouts. Sprouting endothelial cells degrade their basement membrane by production of matrix metalloproteinases (MMPs) [1, 2] as well as over-production of extracellular matrix proteins [3, 4], and form contacts with and migrate along extracellular matrix components [5], resulting in vessel elongation. Later, endothelial cells deposit a new basement membrane resulting in a patent, perfusion-capable capillary [6]. The process of angiogenesis is fundamentally important to the formation of new vasculature during development [4, 7-9], wound healing [10-13] and tumorigenesis [6, 14-18]

Elucidation of the mechanisms controlling microvessel sprouting and the interaction of microvessels with the ECM has basic scientific interest and potential clinical application. However, when attempting to clarify the contribution of the many processes that regulate angiogenesis, one is faced with the insuperable task of attempting to isolate the individual contribution of many inter-related biological processes. Although angiogenesis has been studied extensively in the context of disease and injury (e.g., [10, 14, 15, 19]), little is known regarding the fundamentals of vessel sprouting and elongation in a three

dimensional environment. Recent studies have demonstrated that biophysical aspects of the ECM can be as important as molecular signals in modulating angiogenesis [20-23]. Thus, characterization of the interactions between microvessels and the surrounding ECM would provide new insight into the mechanistic basis of tissue organization and its role in development, disease and soft tissue injury/healing. This will not only further our basic understanding of angiogenesis, but will also provide design principles that may be exploited to engineer patterned microvascular constructs with specific vessel topology.

Tissue and organ mimics such as 3D in vitro models provide a unique, highly controllable paradigm for studying the physiology and pathophysiology of human tissues. In vitro models of angiogenesis based on isolated cells often do not recapitulate realistic sprouting and elongation. Interpretation of results is further complicated by the possibility of cell lineage specific behavior in the model. Our 3D in vitro model of angiogenesis is based on isolation and culture of microvessel fragments in a 3D collagen gel matrix [24-28], and is most accurately described as an "organ culture" model. Unlike other 3D in vitro models of angiogenesis that begin with isolated endothelial cells, our model uses isolated microvessel fragments that include the full spectrum of vessel elements in the microvasculature, namely arterioles, capillaries and venules [24]. These "parent" vessels contain associated perivascular cells [24] and retain their basement membrane after initial harvest and seeding. Pericytes disassociate from the parent vessels and the endothelial cells. This phenomenon is consistent with the increasingly recognized role of pericytes in angiogenesis and observations that perivascular cell withdrawal from vessel segments relaxes the parent endothelial cell tube and permits sprouting and vessel elongation

during angiogenesis [29-33]. Sprouts elongate as patent tubes, branching and anastamosing with other vessels. New neovessels continue to grow into a new vascular network that ultimately fills the gel space by Day 10 of culture. These neovessels form a functional vascular tree when implanted [28] - microvascular constructs cultured for 7 days rapidly inosculate with the recipient host circulation after implantation and begin to carry blood. This demonstrates that neovessels formed via angiogenesis in the collagen gels remain perfusion competent and capable of progressing into a perfused network. Construct implantation allows the study of post-angiogenesis events.

Collagen crosslinking

Background and Motivation

In an effort to understand collagen remodeling during angiogenesis, experiments were proposed in which collagen crosslinks were to be induced in three separate manners, glycation, transglutaminase, and lysyl oxidase. The intent of the experiments was to evaluate the endogenous optical signatures of the different crosslinking schemes using fluorescence spectroscopy as well as two-photon excited fluorescence (2PEF) and second harmonic generation (SHG). Development of endogenous optical signatures of crosslinked collagen would allow us to evaluate the extent of collagen crosslinking within a live sample thereby providing us a way to evaluate crosslinking without destruction of the sample which is the current standard of evaluation using chemical, enzymatic or mechanical means. Spectroscopy on collagen cross links has been previously used to quantify their presence with high pressure liquid chromatography [34], but to our knowledge no attempts were made to incorporate these techniques into laser scanning microscopy, perhaps due to the challenge of UV-excitation. **Table 1** illustrates the known

fluorescence emission properties for collagen cross links which suggests the complexity of collagen fluorescence.

Cross Link Type	*Cross Link*	Excitation max	Emission max	Fluor. Contrib.	Proposed Excitation
Immature Enzymic Reducible	Lysinonorleucine (LNL)	350	400		2PEF
Immature Enzymic Reducible	Hydroxylysinenoro-leucine (HLNL)	350	400		2PEF
Immature Enzymic Reducible	Dehydrocylysineoroleucine (DHLNL)	350	400		2PEF
Mature Enzymic Hystidine	Histidino-hydroxylysinonor-leucine (HHL)	unkwn	unknwn		2PEF
Mature Enzymic Pyrrole	Pyridinium: Lysyl-**pyridinoline** (L-Pyr)	325 (290)	400 (380-460)		3PEF
Mature Enzymic Pyrrole	Pyridinium: Hydoxylysin pyridinoline (H-Pyr)	325 (290)	400		3PEF
Glycation	**Pentosidine**	335	385	25-40%	3PEF
Glycation	Vesperlysine A, B, C	370	440	5%	2PEF
Glycation Lysine	Crossline A, B	380	460		2PEF
Glycation Arginie	Argpyrimidine	320	380		3PEF

Table 1: Known fluorescence collagen cross links with their excitation and emission maxima.

Tissue engineering approaches have been successful in providing histochemical as well as biochemical mimicry of certain tissue types including vessels [35-38], nerves [39], skin [40-43], cartilage [44, 45], bone [46] and ligaments [47]. Scaffolds have been developed with the motivation that seeded materials have a support system which provides cells with growth and migrational support as well as structural context. Since collagens are the primary component of tissues such as bone, skin, cartilage and tendons, they have been used extensively in biomedical tissues, particularly scaffolds. Collagen scaffolds have been successful but have suffered from issues related to lack of mechanical strength. Crosslinking of collagen is one way to increase the mechanical strength of collagen and has been described by many methods. Ultraviolet light [48-50], dehydrothermal treatment [50], chemical agents such as glutaraldehyde [48, 51-54], acyl azides [55], other chemical means [56-62], non-enzymatic glycation [57], enzymatic crosslinking by transglutaminase [63, 64] and overexpression of the crosslinking enzyme lysyl oxidase [65, 66] are among the techniques utilized. When considering the various

crosslinking techniques, one must consider the potential effects of cytotoxicity as a result of the agent used. Glutaraldehyde was shown to impart some degree of cytotoxicity when crosslinked prior to cell seeding [67] while transglutaminase [63, 64], lysyl oxidase [65, 66] and glycation [57] showed no apparent cytotoxicity. The latter three methods are the only ones currently accepted as non-cytotoxic in the presence of cells [57, 63-66].

Glycation

Type I rat tail collagen (BD Biosciences, San Jose, CA) was utilized in a final concentration of 3mg/mL. 1.327mL collagen was combined with .2mL of 10X Hanks medium for a final concentration of 1X Hanks, 20mM HEPES and .433mL sterile water for a final volume of 2mL. The mixture was then pH neutralized using 1M NaOH, loaded into 48 well plates (200μL per gel) and incubated at 37°C for 30 minutes to polymerize the gels. Standard M199 reagent (GIBCO, Grand Island, New York), which has a glucose concentration of 5mM, was used in wells 1 and 2 as controls. Wells 3 and 4 were supplemented with 15mM glucose in M199, wells 5 and 6 with 30mM glucose in M199, and wells 7 and 8 with 50mM glucose in M199. The gels were allowed to incubate at 4°C for 7 weeks. After 7 weeks, the samples were removed from the 48 well plates and placed in a quartz imaging chamber and subjected to fluorescence spectroscopy.

Fluorescence spectroscopy. The fluorescence properties of the collagen gels were measured in a standard 1 cm path length quartz cuvette using a double excitation emission fluorometer (Fluorolog 3-22, JY Horiba, Edison, NJ). For each spectroscopic experiment, excitation and emission wavelengths were varied to obtain fluorescence data

matrices. Excitation wavelengths varied from 270 to 600 nm in increments of 10 nm while collecting emission data from a range starting 20 nm above the excitation wavelength and extending to 20 nm less than twice the excitation wavelength with 700 nm as the maximum measured emission wavelength. Each measurement takes approximately 15 min to complete. Each of the three conditions was measured only once due to technical difficulties extracting the samples from the 48 well plates. The gels either tore or were stuck inside the wells. Speculation is that, either length of time or glucose content or the combination of both, allowed the gels to bond with the plastic surface of the wells. Also, when imaging was performed, the gels were slightly compacted in order to fit within the imaging chamber which would lead to changed optical characteristics as well as inconsistency. Excitation emission matrices (EEMs) showing the results of the three scans alone and relative to each other are shown in **Figure 1**. Preliminary analysis showed no prominent distinction between the samples but did show a slight difference between the 15mM scan and the 25mM scan. Since we did not have the requisite amount of scans for statistical analyses, we elected to continue with a second experimental protocol. We elected to mold the gels while in the imaging chamber itself then remove the gels and suspend them in the desired media. The gels were approximately 1mm thick but proved to be too thin to transfer back into the imaging chamber intact after 8 weeks of incubation time resulting in no measurements being taken using this setup.

Transglutaminase

Type I rat tail collagen (BD Biosciences, San Jose, CA) was utilized in a final concentration of 3mg/mL. 1.327mL collagen was combined with .2mL of 10X Hanks medium for a final concentration of 1X Hanks, 20mM HEPES and .433mL sterile water for a final volume of 2mL. The mixture was then pH neutralized using 1M NaOH, loaded into 48 well plates (200μL per gel) and incubated at 37°C for 30 minutes with a 5000:1 ratio of collagen to transglutaminase enzyme as per previous work done by Orbam et al [64]. Recombinant human transglutaminase (rhTG2 (N-ZYME Biotech GmbH, Darmstadt, Germany)) was determined to be suitable for our purposes after correspondences to N-ZYME Biotech and was added prior to incubation. The gels were then analyzed using fluorescence spectroscopy within a few hours of polymerization.

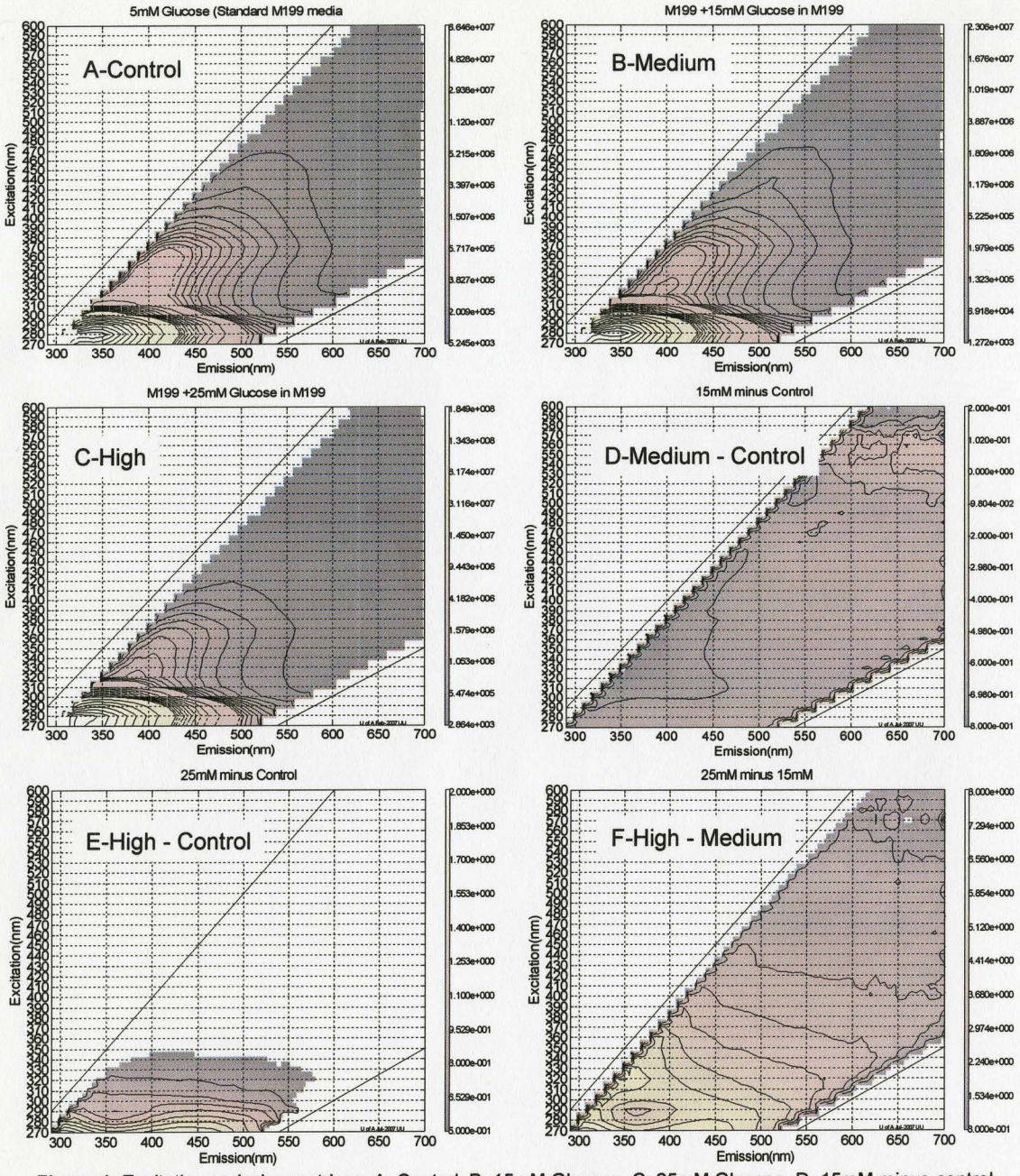

Figure 1. Excitation emission matrices. A: Control. B: 15mM Glucose. C: 25mM Glucose. D: 15mM minus control. E: 25mM minus control. F: 25mM minus 15mM.

UV quartz imaging (inset) chambers were obtained (NSG Precision Cells, Farmingdale, NY). The chamber volume is 360μL with a 1mm light path, inner length of 38mm, and inner width of 10mm. The imaging chamber has a detachable quartz cover. A schematic of the chamber is shown to the right. Collagen gels were polymerized at 37°C directly in the imaging chambers. For this study we used a collagen minus and rhTG2 (recombinant human transglutaminase 2, N-Zyme Biotech, Darmstadt, Germany) minus negative control in addition to an rhTG2 minus negative control. The experimental group was rhTG2 positive. The collagen$^-$ /rhTG2$^-$ control was measured with n = 3, the rhTG2$^-$/collagen$^+$ control was measured with n = 3 while the rhTG2$^+$ /collagen$^+$ experimental condition was measured with n = 7. Mean EEMs of each group of scans are shown in **Figure 2, A-C** while differences in means plots are shown in **Figure 2, D-F**.

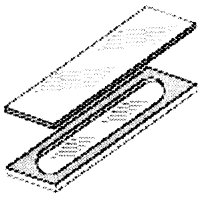

Extensive data analysis was performed to try and identify differences in optical signatures at numerous excitation and emission wavelengths. The overall conclusion was that there were not significant differences identified between the three groups for further development using endogenous fluorescence signatures. We then tried using multiphoton microscopy to see if we could identify qualitative differences between the collagen$^+$/rhTG2$^-$ and collagen$^+$/rhTG2$^+$ groups. The samples were imaged with a 150 fs pulsed titanium-sapphire laser (Mira 900, Coherent, Santa Clara, CA) coupled to a laser-scanning confocal microscope (LSM 510, Carl Zeiss, Jena, Germany). Incident light was focused and emitted signals were collected with a 40X 1.3 NA oil immersion objective (Carl Zeiss). The laser was centered at either λ_{inc} = 720 nm or λ_{inc} = 780 nm and 2PEF

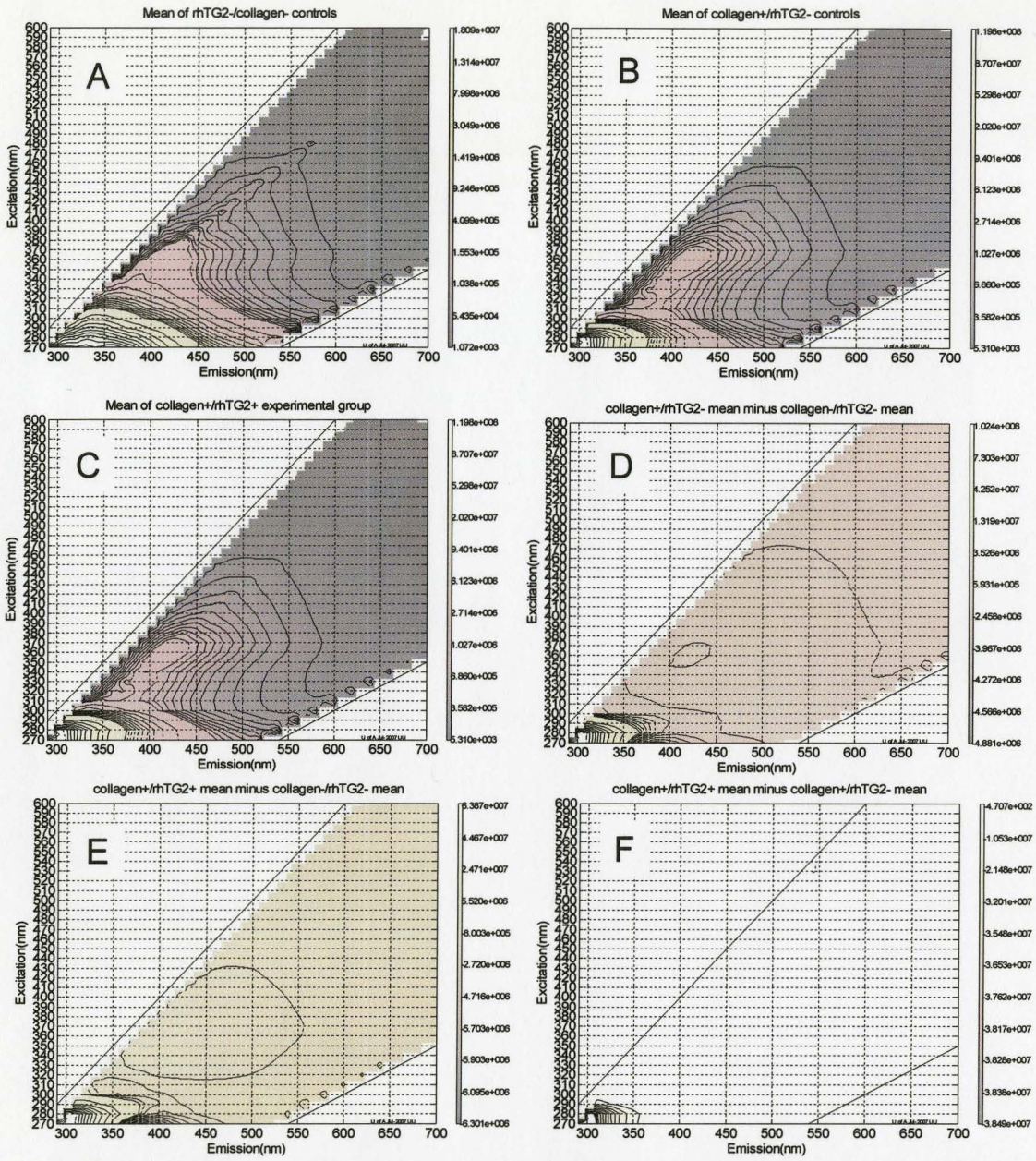

Figure 2. Excitation emission matrices. A: Mean of collagen$^-$/rhTG2$^-$ controls (n=3). B: Mean of collagen$^+$ rhTG2$^-$ controls (n=3). C: Mean of collagen$^+$/rhTG2$^+$ experimental group (n=7). D: Mean of collagen$^+$/rhTG2$^-$ minus mean of collagen$^-$/rhTG2$^-$. E: Mean of Colagen$^+$/rhTG2$^+$ minus mean of collagen$^-$/rhTG2$^-$. F: Mean of collagen$^+$/rhTG2$^+$ minus mean of collagen$^+$/rhTG2$^-$.

signals were collected in the epi-fluorescence configuration through a custom multiphoton filter (480 – 580 nm, Chroma, Rockingham, VT) and onto a non-descan PMT detector (based on R6357, Hamamatsu, Hamamatsu City, Japan). Similarly, the SHG signal was collected onto a second non-descan PMT detector through a custom SHG filter (380 – 400 nm, Chroma). We concluded that there was not a significant difference in 2PEF to be useful for detecting differences in collagen crosslinking. In addition, evaluation of the crosslinking extent using SHG did not prove fruitful as expected due to lack of evidence of differences using fluorescence spectroscopy. The collagen gels were also quite inconsistent in makeup. **Figures 3-6** show representative fields of view illustrating which proved to make it difficult to note differences between the groups evaluated. One might argue that there are differences in the images shown, however, we could not rule out experimental issues such as temperature, compression of the gels, time exposed to laser light etc. An interesting phenomenon that we observed while performing SHG on the samples in that the 2PEF observed increased dramatically as the samples were exposed to room temperature for longer periods of time (**Figure 7**). There appears to be significant co-localization of the 2PEF signal and the SGH signal which might indicate increased crosslinking as a result of the longer exposure time to the laser, cooling to room temperature or some other unforeseen phenomenon. As a consequence of this observation, the experiment could be repeated in a more controlled manner that accounts for experimental factors.

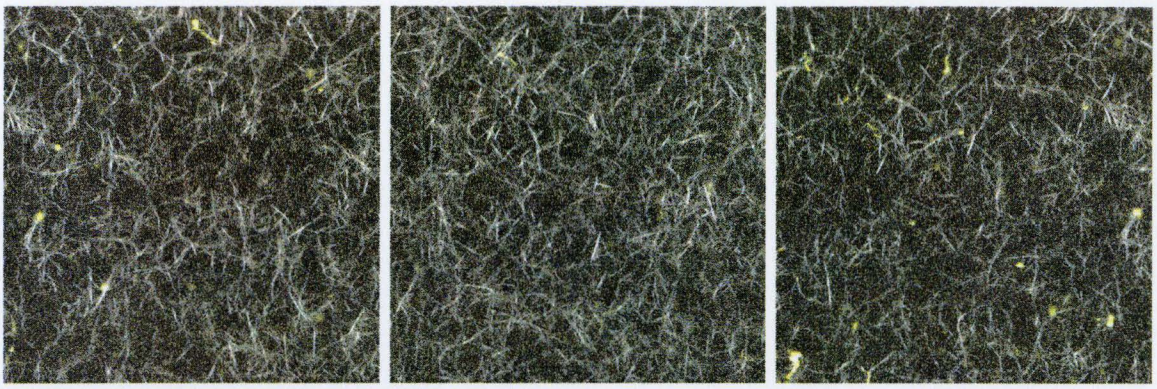

Figure 3. Collagen^{+}/rhTG2^{-} 720nm excitation, 40x objective, zoom factor 2

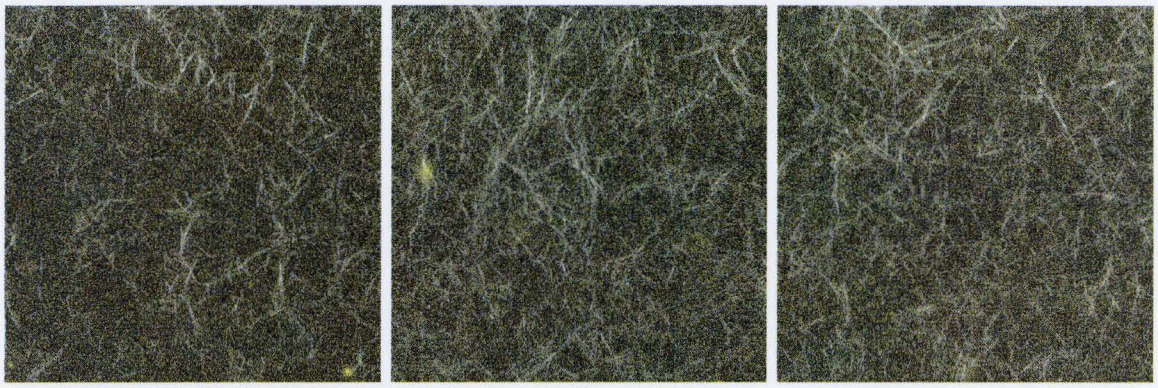

Figure 4. Collagen^{+}/rhTG2^{+} 720nm excitation, 40x objective, zoom factor 2

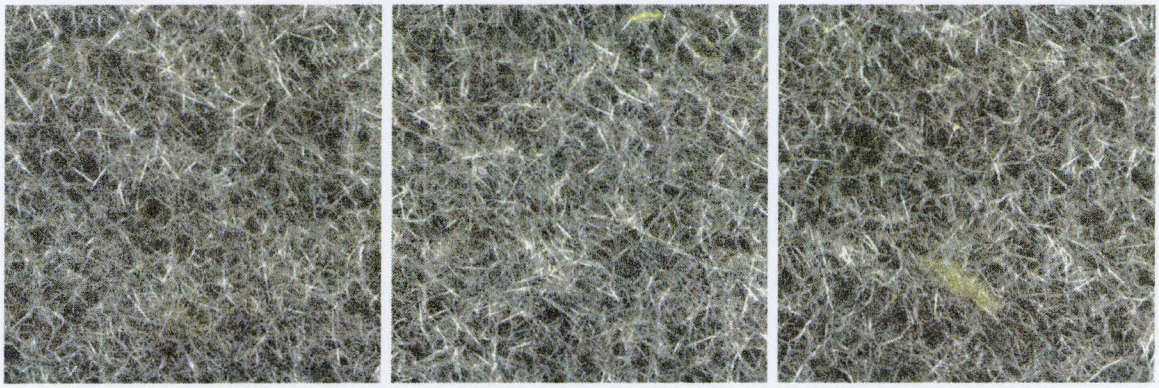

Figure 5. Collagen^{+}/rhTG2^{-} 780nm excitation, -40x objective, zoom factor 2

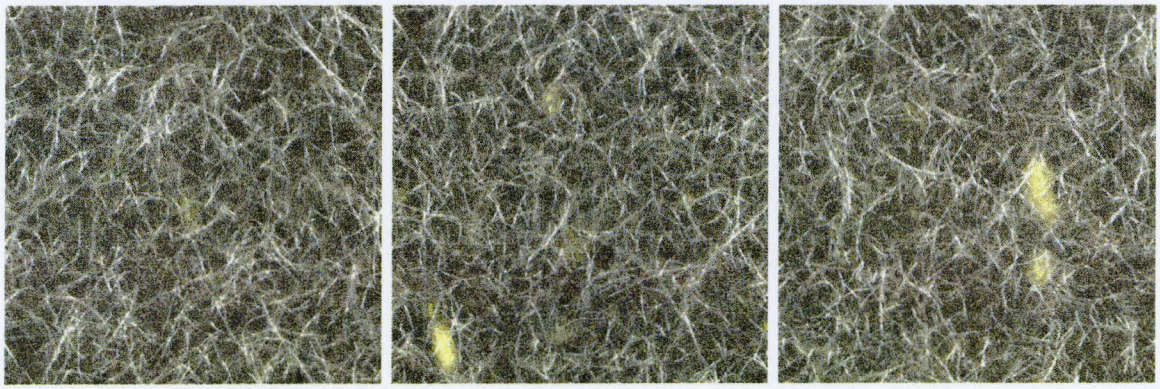

Figure 6. Collagen^{+}/rhTG2^{+} 780nm excitation, 40x objective, zoom factor 2

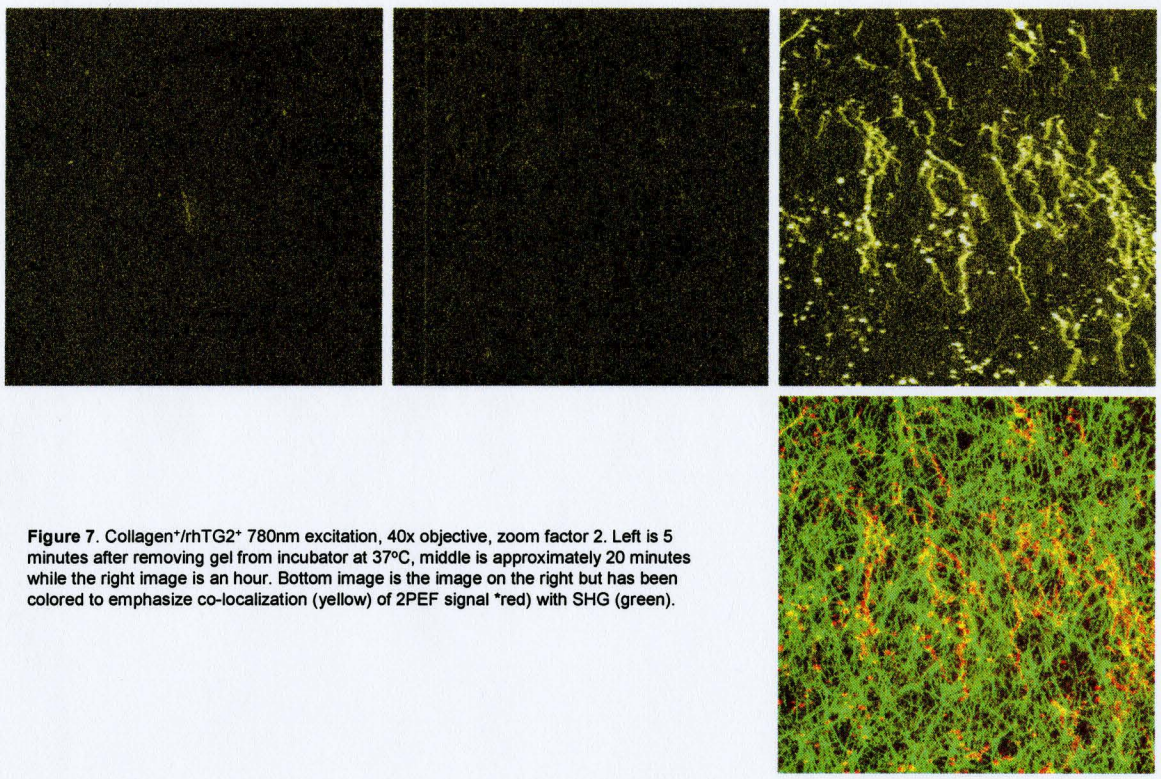

Figure 7. Collagen^{+}/rhTG2^{+} 780nm excitation, 40x objective, zoom factor 2. Left is 5 minutes after removing gel from incubator at 37°C, middle is approximately 20 minutes while the right image is an hour. Bottom image is the image on the right but has been colored to emphasize co-localization (yellow) of 2PEF signal *red) with SHG (green).

Future Directions

A third method of collagen crosslinking involves enzymatic crosslinking of collagen based on the overexpression of lysyl oxidase. Lysyl oxidase overexpressing cells can be obtained as previously described [65]. Briefly, human lysyl oxidase clone (OriGene, Rockville, MD) are cloned into a commercially available mammalian vector, PCMV6-XL% (OriGene). Vascular smooth muscle cells are seeded into 6-well plates at a concentration of 75,000 cells per well. Twelve hours following seeding, 3μL of FuGENE 6 cationic liposome formulation (Roche Biochemical, Indianapolis, IN) is added to 100μL of serum-free DMEM (GIBCO, Grand Island, NY) and allowed to incubate at room temperature for 5min. 3μg of plasmid DNA is added to the mixture and allowed to incubate at room temperature for 15 min. The Fugene 6/DNA complex is added to each well. Cells are incubated with Fugene 6/DNA complex for 9 hours at which time fresh

medium is added. As a control, seeded wells receive the plasmid DNA vector with no lysyl oxidase cDNA. Culture media is collected and used to supplement standard media when culturing micro vessel constructs. This experimental design is inherently less clean than being able to add a purified enzyme directly to the gels as in the transglutaminase procedure so care would need to be taken to control for this and while interpreting data obtained from such experiments.

Further experiments could be done with glycation to definitively determine if there indeed is no endogenous fluorescence signatures associated with crosslinking of collagen by either method. Since molding the gels in the imaging chamber and then removing them proved problematic, one might devise a strategy in which a custom imaging chamber was manufactured which is significantly thicker, at least 2mm which would be an improvement over the existing 1mm thickness from current imaging chambers. With this approach, one could incubate the gels in the appropriate media for weeks and the gels should be strong enough to be placed back into the imaging chamber for spectroscopy. In addition, mechanical testing might be utilized to help determine if crosslinking had occurred via increased mechanical strength.

Future work for transglutaminase crosslinking could be performed by utilizing mechanical testing methods to determine if the transglutaminase procedure is working. We used a procedure which had been reported to increase the mechanical properties via transglutaminase crosslinking [64], however, we do not have proof that the technique actually crosslinked our collagen gels. As a consequence, our negative results may be due

to experimental error. For simplicity, one could also use any of the available chemical assays for validation of the experimental protocol as well.

MMP: Localization

Background and Motivation

Matrix metalloproteinases (MMPs) are a large family of enzymes which regulate the extracellular matrix (ECM) composition. Between the >25 MMPs identified to date, virtually any component of the ECM can be cleaved [68]. All MMPs contain a propeptide and a zinc catalytic domain as well as a conserved methionine [69]. MMPs along with their inhibitors and activators are heavily studied and have been shown to be involved in numerous aspects of cancer biology, recent references [70-75]. MMPs are also linked to angiogenesis which is one of the hallmarks of cancer [70-76]. Our intent is to study angiogenesis and not necessarily cancer, which are often linked as can be seen in the previous references. Several models exist to test angiogenesis which is defined as the growth of new blood vessels from pre-existing vessels. Most early work was performed in cell culture while more recent work has utilized methods such as the mouse aortic ring model [77-80], culturing endothelial cells within three-dimensional fibrin gels [81], or the use of microvessel fragments suspended within a three-dimensional collagen lattice [24, 28]. It has been thought that MMP-2 and MMP-9 play an important role in angiogenesis and there is abundant evidence in the literature which supports this. In addition to MMP-2 and MMP-9, other MMPs are being linked to angiogenesis including MT1-MMP (MMP-14) which is emerging as a potentially major player in angiogenesis [77, 81, 82]. Molecular methods have shown the presence and activity of MMP-2, MMP-9 and MT1-

MMP but, to our knowledge, there have been no studies which show localization of the respective MMPs or localization of their respective activity. Using the microvessel fragment model, we can visualize localization of the MMPs of interest using *en bloc* immunostaining and fluorescence confocal microscopy.

Results

Microvessel constructs were stained at various timepoints within the range in which the constructs actively sprout and elongate (day 3 through day 10). We anticipated a differential expression of the MMPs involved based on preliminary data by the Hoying lab which performed DNA microarray analysis illustrating a change in gene expression of both MMP-2 and MMP-9 (unpublished data). The constructs were stained by en bloc immunostaining according to the protocol developed by our lab (See Appendix). Since we wanted to visualize all three of the chosen MMPs at once, we needed to choose our stains carefully to avoid spectral overlap of the fluorescence signals. We settled on Alexa Flour 488, 546, and 647 (Molecular Probes, Eugene, OR) with excitation/emission spectra shown in **Figure 8**. MMP-14 was stained with Alexa Fluor 488, MMP-2 with Alexa Fluor 546 and MMP-9 with Alexa Fluor 647 for all experiments.

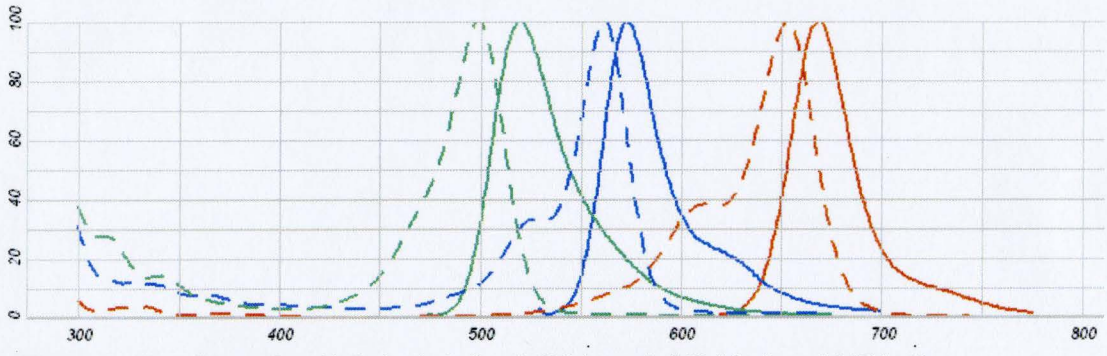

Figure 8. Alexa fluor ex/em (dotted, whole lines) 488 (green), 546 (blue), and 647 (red)

Day 3 constructs should show limited if no sprouting at all. Day 3 staining showed the presence of all three MMPs while vessel sprout had not yet begun (**Figures 9**). MMP-14 is shown in blue, MMP-2 is shown in green and MMP-9 in red. MMP-14 and MMP-2 are present to a much greater degree than MMP-9 but one cannot say much about this as the lasers were tuned in such a way as to maximize the signal from each without saturating the detectors which does not account for quantum efficiency of the fluorescence tag. SHG shows condensation around the microvessel fragments consistent with work done previously [25]. One of the pitfalls of the immunostaining protocol is the use of Triton X100 which is a detergent that permeabilizes the membranes of cells which leads to the potential staining of internal stores of MMPs. This is most likely the cause of the majority of fluorescence signals generated. Speculation is that the MMPs are not concentrated enough in one area in the surrounding matrix to stain effectively. Studies were planned in which Triton X100 was omitted but have not been performed to date. Day 4 is when the constructs should just be starting to sprout. Staining of day 4 constructs showed concentration of MMP-14 and MMP-9 along the border of the microvessel fragment while MMP-2 remained diffuse within the boundaries of the fragment.

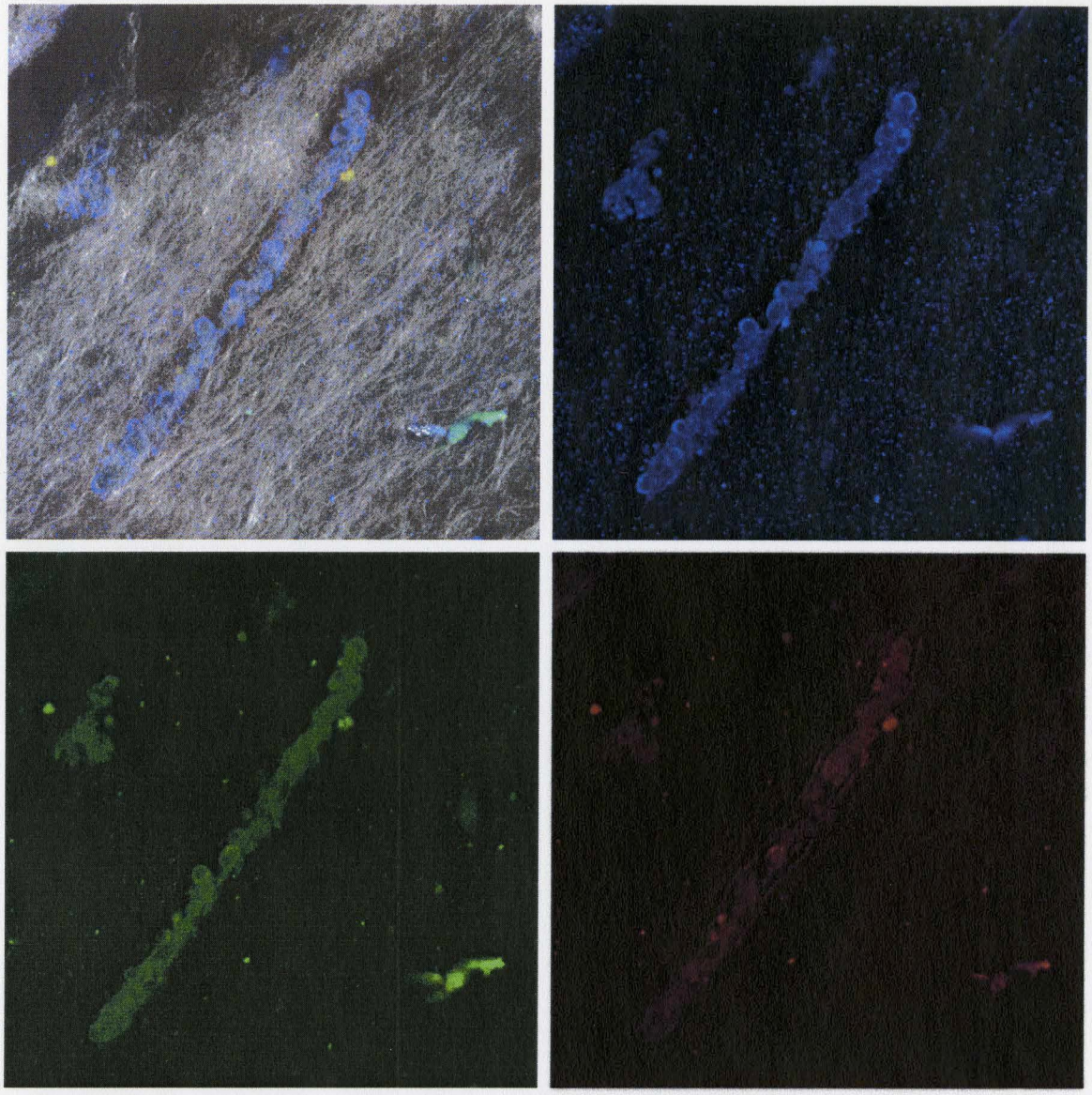

Figure 9. Day 3 construct staining. Upper left, combined MMP-14 (blue), MMP-2 (green), MMP09 (red), SHG (white). Upper right, MMP-14, Lower left, MMP-2, Lower right, MMP-9.

SHG on day 4 constructs was much as it was on day 3, condensed along the border of the microvessel fragment. An interesting phenomenon in which very thin protrusions of the membrane was noted which only stained for MMP-14. We have speculated that these protrusions are filopodia which are extending into the matrix in an effort to identify the best route for extension of a neovessel sprout. We have noted this only in day 4 constructs suggesting that this is an early event in sprouting using our model. Upon close

inspection of the SHG signals in the region of filopodia activity, one can see very thin collagen fibrils that may be aligning with the direction of filopodia as well as in the projected direction of filopodia extension (**Figure 10**).

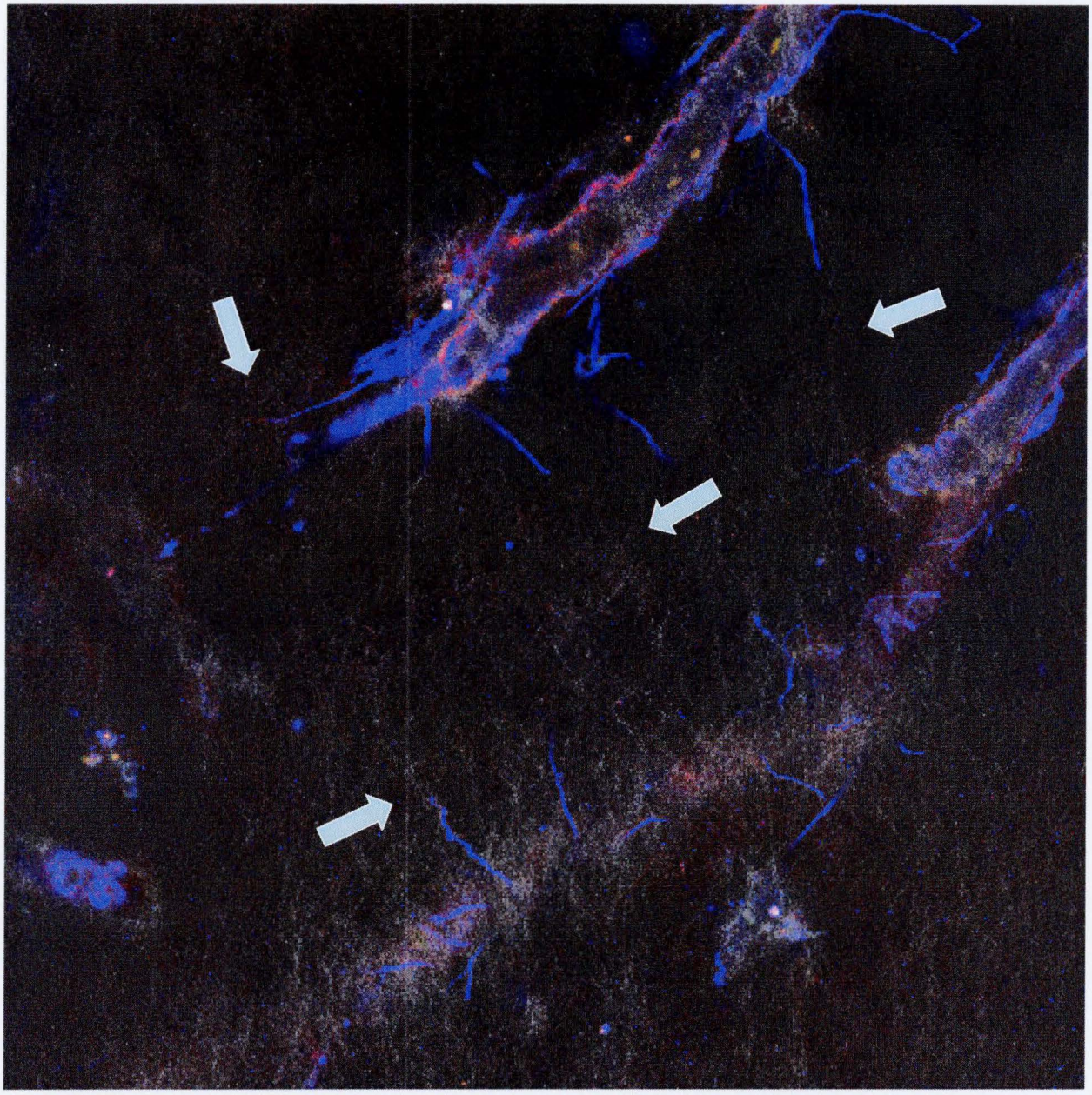

Figure 10. Day 4 construct. Areas indicated by arrows show possible alignment with collagen fibers.

Figure 11 shows what appear to be filopodia interescting between two parent vessel fragments and note that only MMP-14 stains these (**Figure 12**). **Figure 13** shows a similar phenomenon in a separate experiment. One can see that these filopodia are extending in several places from the parent vessels but it is unclear as to whether they are proceeding along collagen fibers or not. Since this seems to be a rare phenomenon, we would like to repeat this experiment with better SHG contrast and without Triton X100. These two changes should help to clarify what is happening.

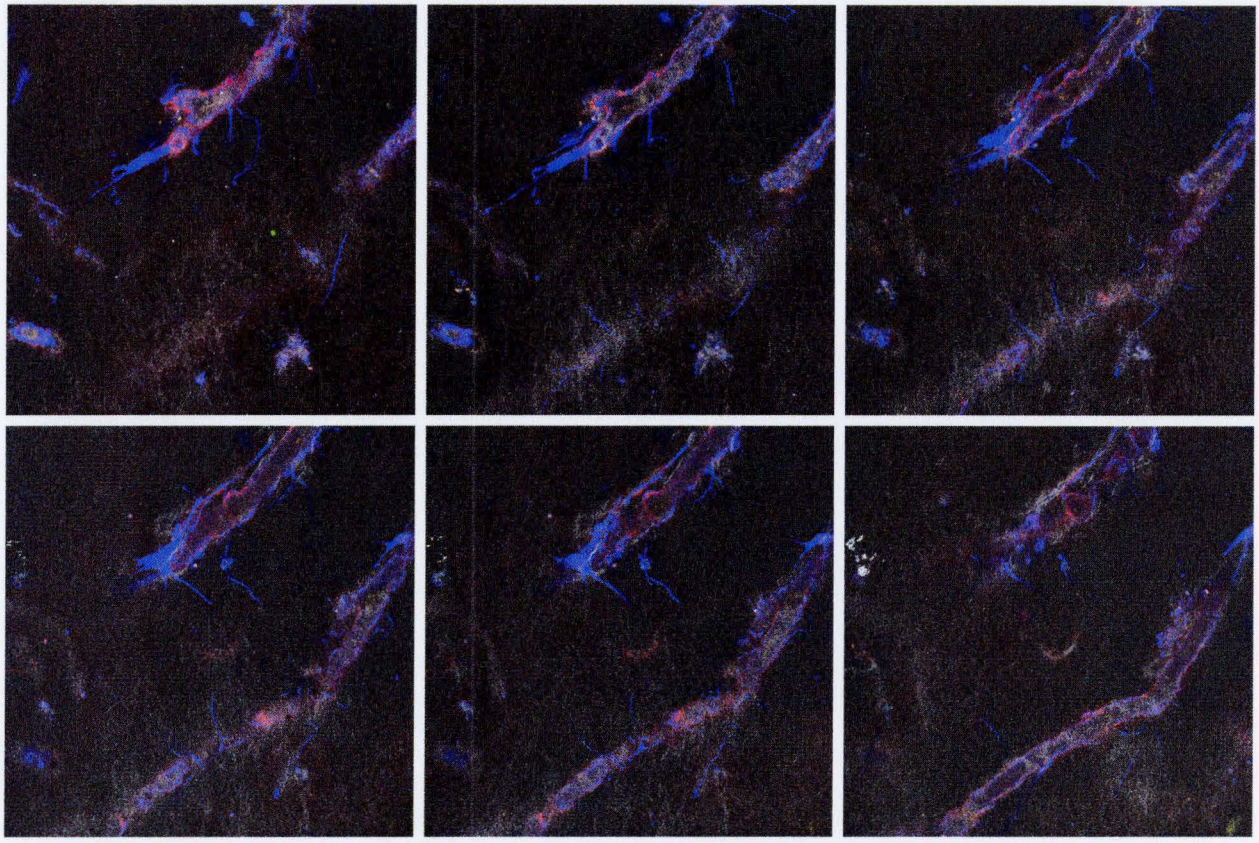

Figure 11. Day 4 construct Z stack which shows the 3D extent of philopodia protruding from two parent vessels. From top left to bottom right is approximately 30μm. Interestingly, some of the philopodia appear to be extending in the direction of the opposite parent vessel.

Day 7 constructs should have abundant sprouting with some which have undergone extension. **Figure 14** shows a day 7 construct illustrating a medium size sprout coming from a parent vessel.

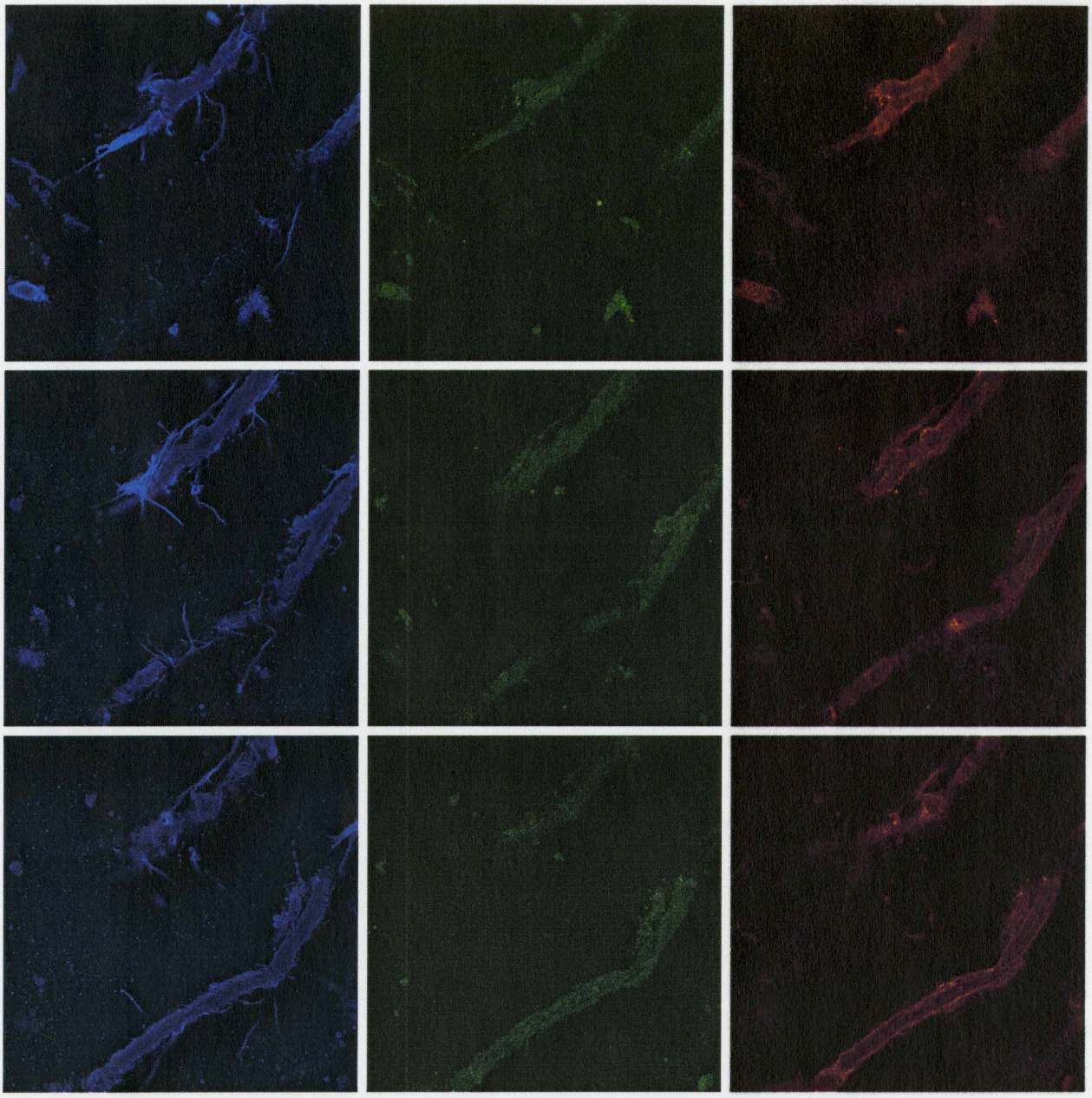

Figure 12. Tricolor staining of day 4 construct MMP-14 (blue), MMP-2 (green), MMP-9 (red) illustrating that only MMP-14 stains the "filopodia".

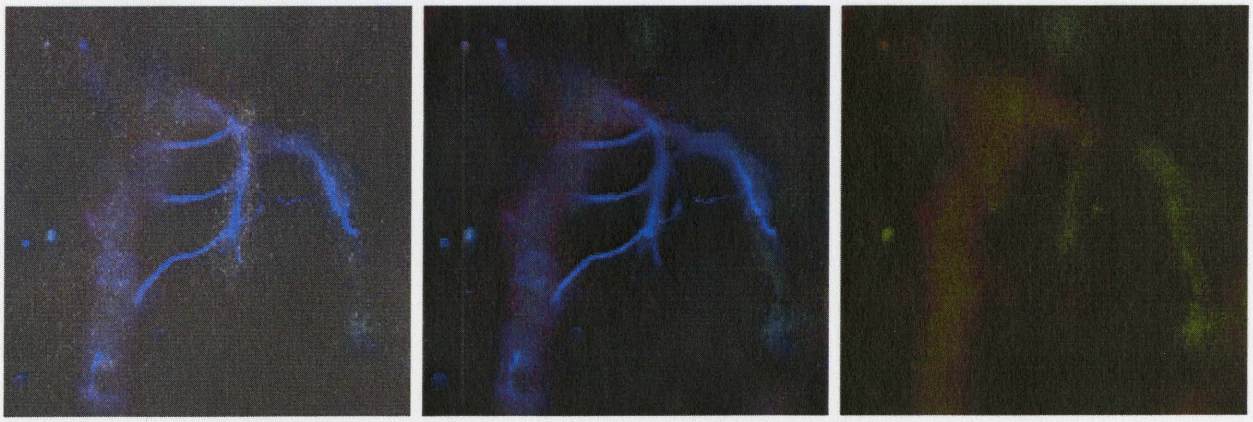

Figure 13. Day 4 construct. Left is combined image with MMP-14, MMP-2, MMP-9 (blue, green, red) and SHG in white. The thin extensions stain for MMP-14 only as indicated by a comparison of the middle image (MMP-14) and the right image (MMP-2 and MMP-9).

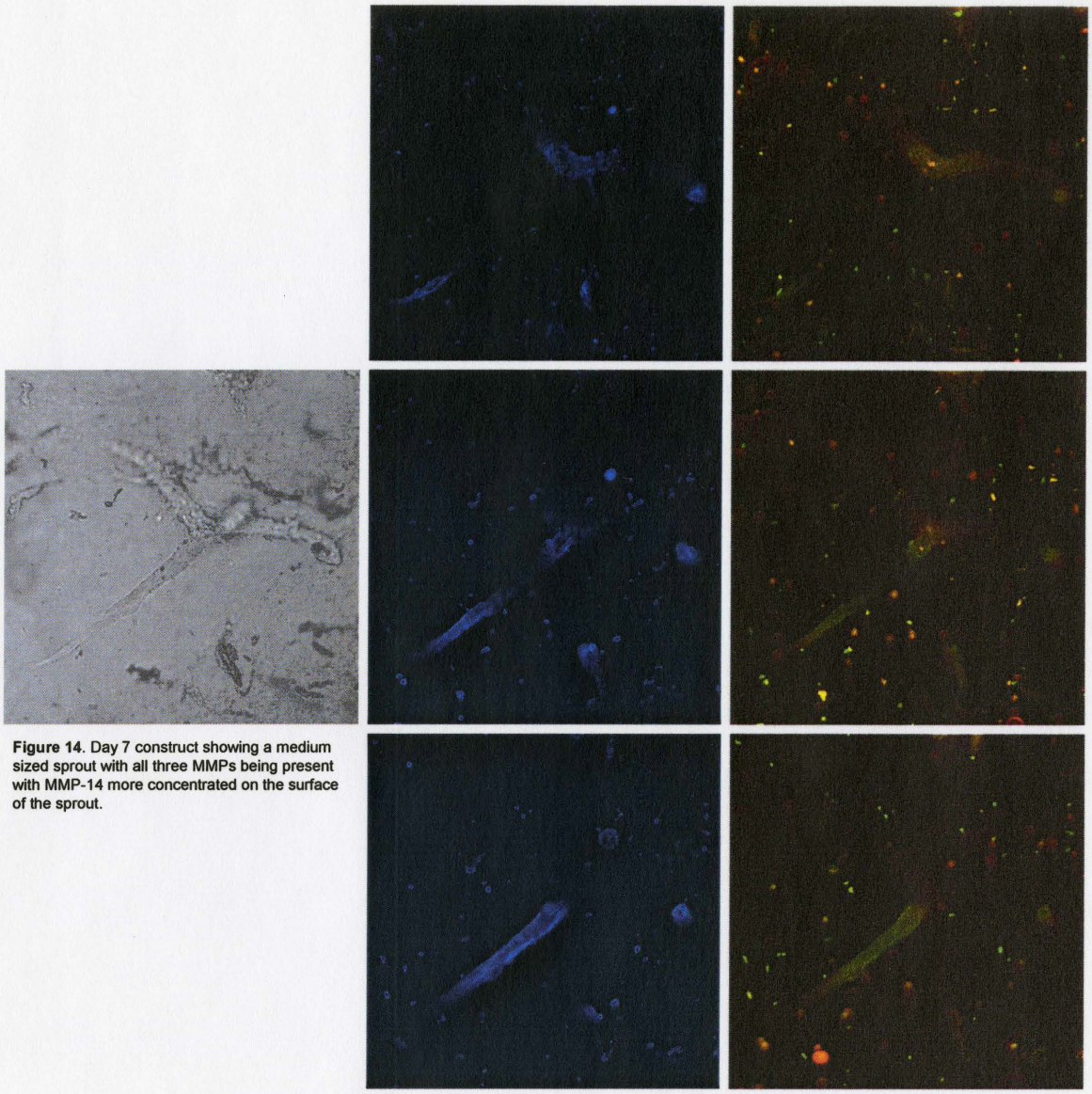

Figure 14. Day 7 construct showing a medium sized sprout with all three MMPs being present with MMP-14 more concentrated on the surface of the sprout.

The sprout shows MMP-14, MMP-2 and MMP-9 staining indicating that all three are involved in the sprouting process. At the very tip of the sprout (**Figure 15**), MMP-14 appears to be present to a much greater degree than either MMP-2 or MMP-9 suggesting MMP-14 may play more of a role in the elongation process than MMP-2 or MMP-9.

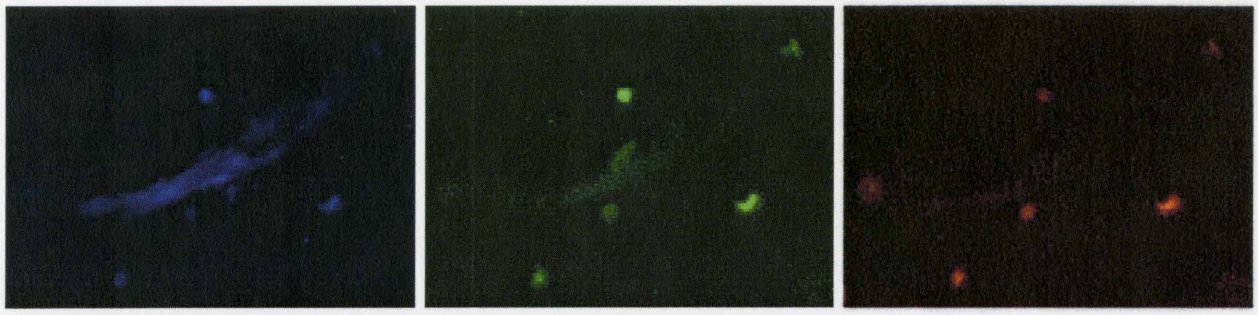

Figure 15. Day 7 construct at sprout tip. MMP-14 (blue) stains stronger than MMP-2 (green) and MMP-9 (red).

Day 10 constructs should have well developed sprouts with some being quite long as well as starting to develop a crude network. We encountered some trouble while staining day 10 constructs. Prior to the staining process the constructs looked well developed, however, after staining the networks failed to show up. This might be contributed to the fixing process or to the staining protocol. **Figure 16** illustrates a day 10 construct with a small network of sprouts as opposed to a well developed network which we expected.

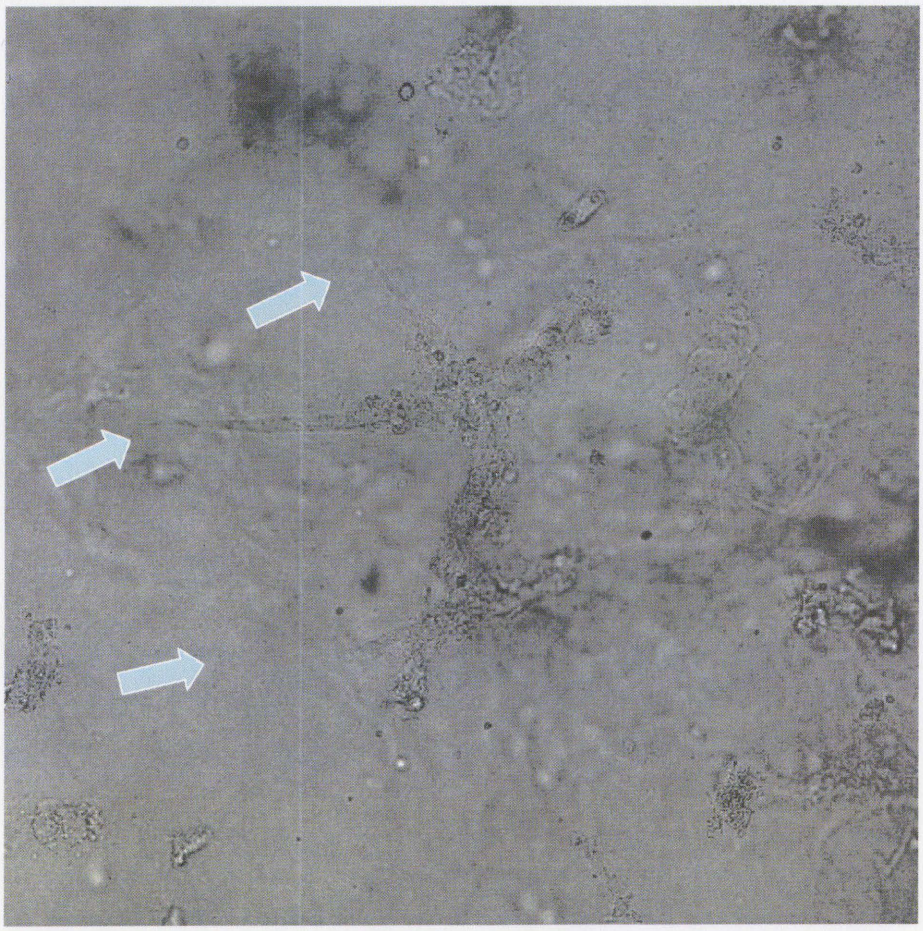

Figure 16. Day 10 construct showing multiple sprouts emerging from either a single or multiple parent vessels which is unclear from the image.

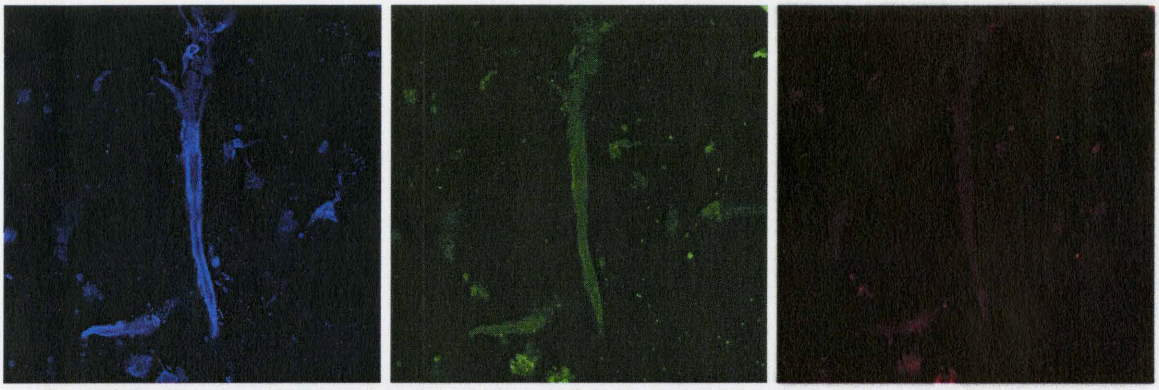

Figure 17. Day 10 construct. Well developed sprout showing Strong MMP-14 (blue) and MMP-2 (green) staining and weak MMP-9 (red) staining.

Figure 17 shows a day 10 construct with a fairly long and well developed sprout. Staining on this sprout shows a large amount of MMP-14 presence as well as MMP-2 but shows little MMP-9. This is of interest as day 3 constructs showed the same staining pattern which might suggest that the well developed sprout is starting to take on an MMP profile that is similar to parent vessel fragments. Also of interest is the observation that MMP-9 is expressed to a much higher degree in day 4 constructs indicating that MMP-9 may be more involved during early sprout formation compared to MMP-2 with MMP-14 staining brightly in all constructs.

Since we hypothesized a differential staining pattern over the time course of the experiments, a comparison of MMP-2, MMP-9 and MMP-14 at key time points was assembled. **Figure 18** shows a comparison between day 3, day 4, day 7 and day 10 MMP-9 staining. MMP-9 appears to be present at low levels at all time points but day 4. A comparison of MMP-2 staining on the same constructs (**Figure 19**) shows that day 4 staining is reduced in comparison to days 3, 7 and 10. Finally, a comparison of MMP-14 staining on the same constructs (**Figure 20**) shows about the equivalent staining pattern in days 3 and 4 which started to become more pronounced by day 7 ending in a much

more pronounced staining of the well developed sprout in the day 10 construct. The significance of these observations is yet to be determined, however, the data do provide encouraging evidence of differential MMP presence along the time points observed.

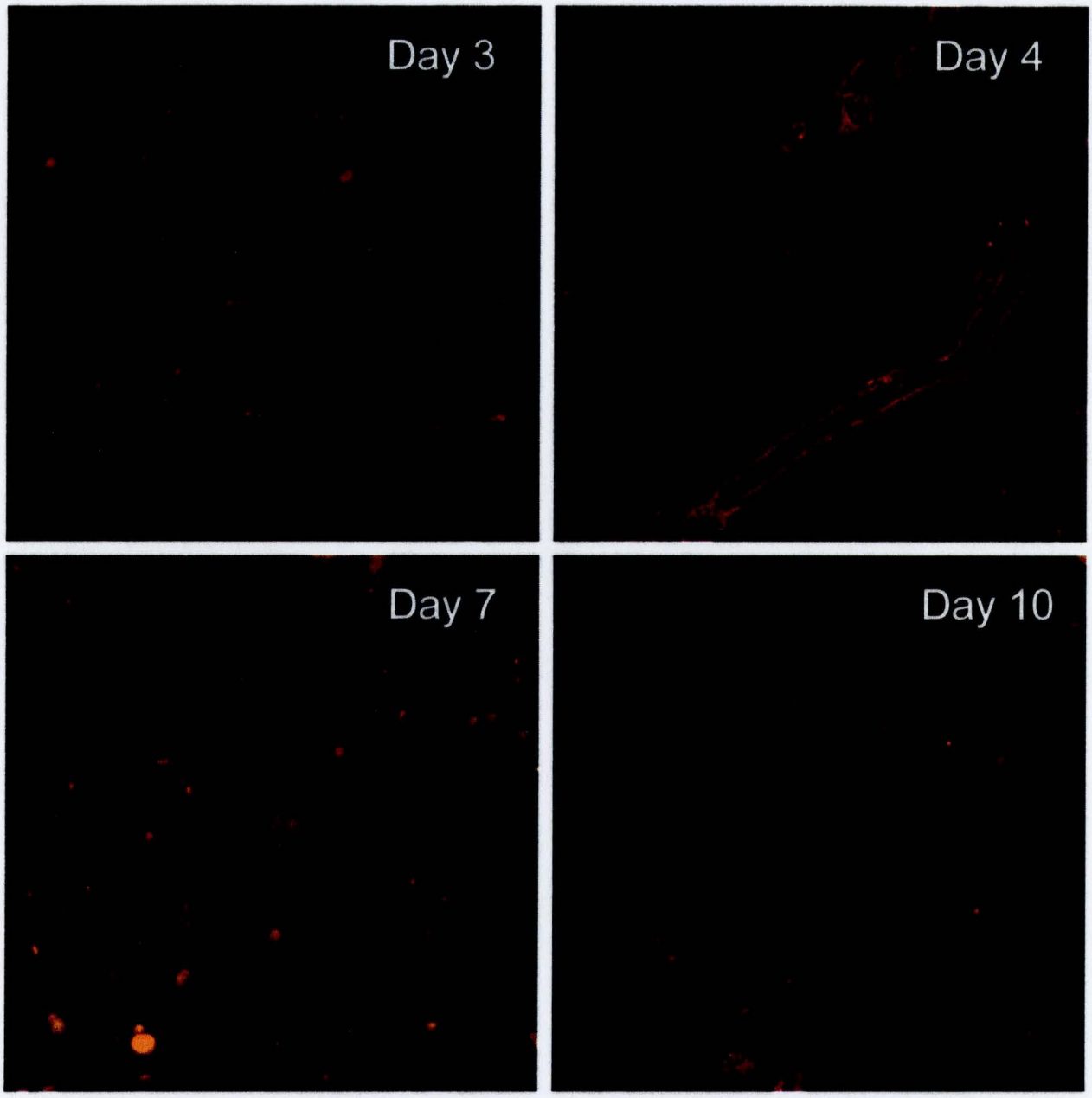

Figure 18. MMP-9 staining patterns of constructs at different times in the sprouting process. Day 4 appears to stain more prominently compared to the other days.

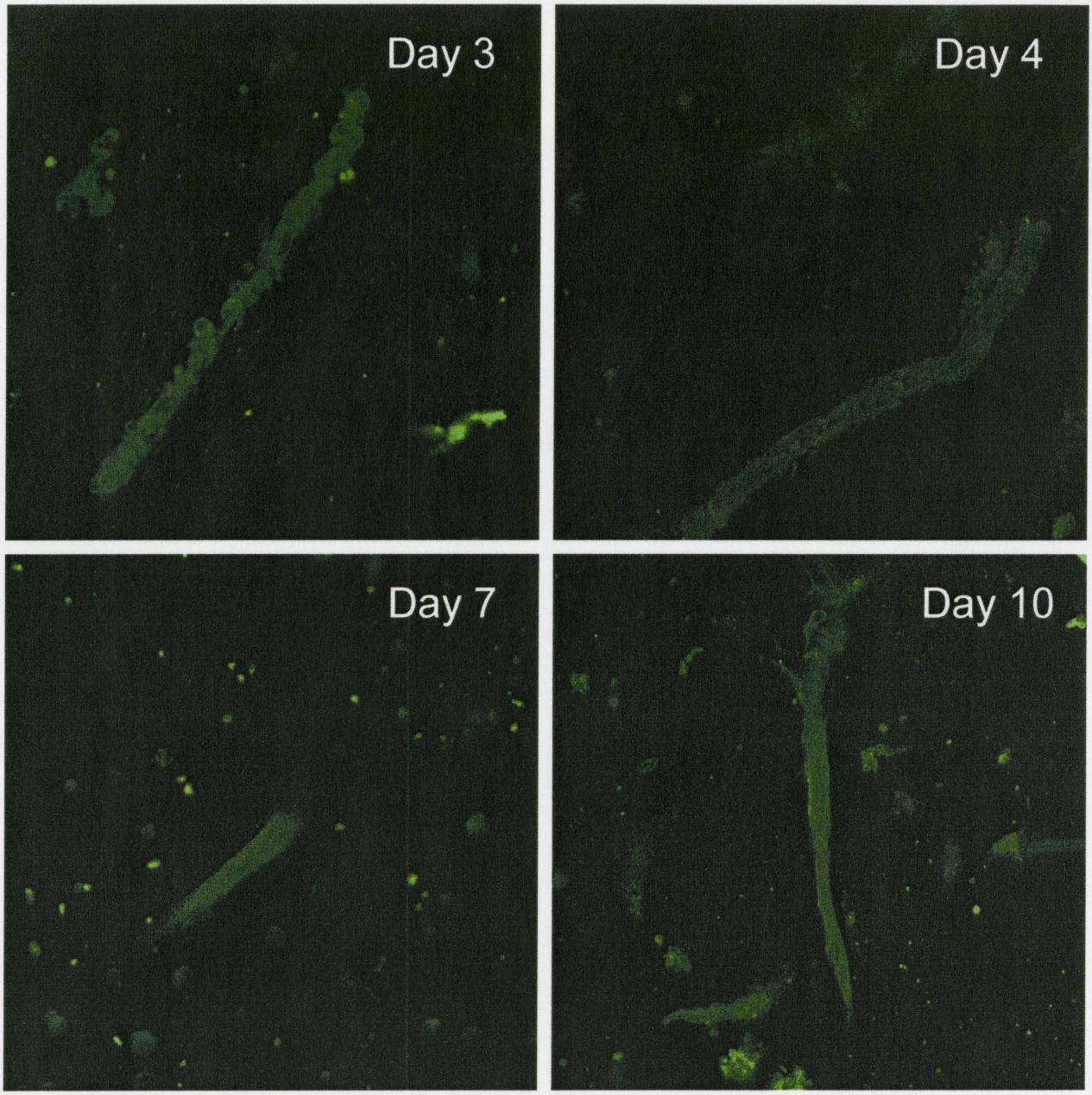

Figure 19. MMP-2 staining patterns of constructs at different times in the sprouting process. Day 4 appears to stain less prominently than the other days.

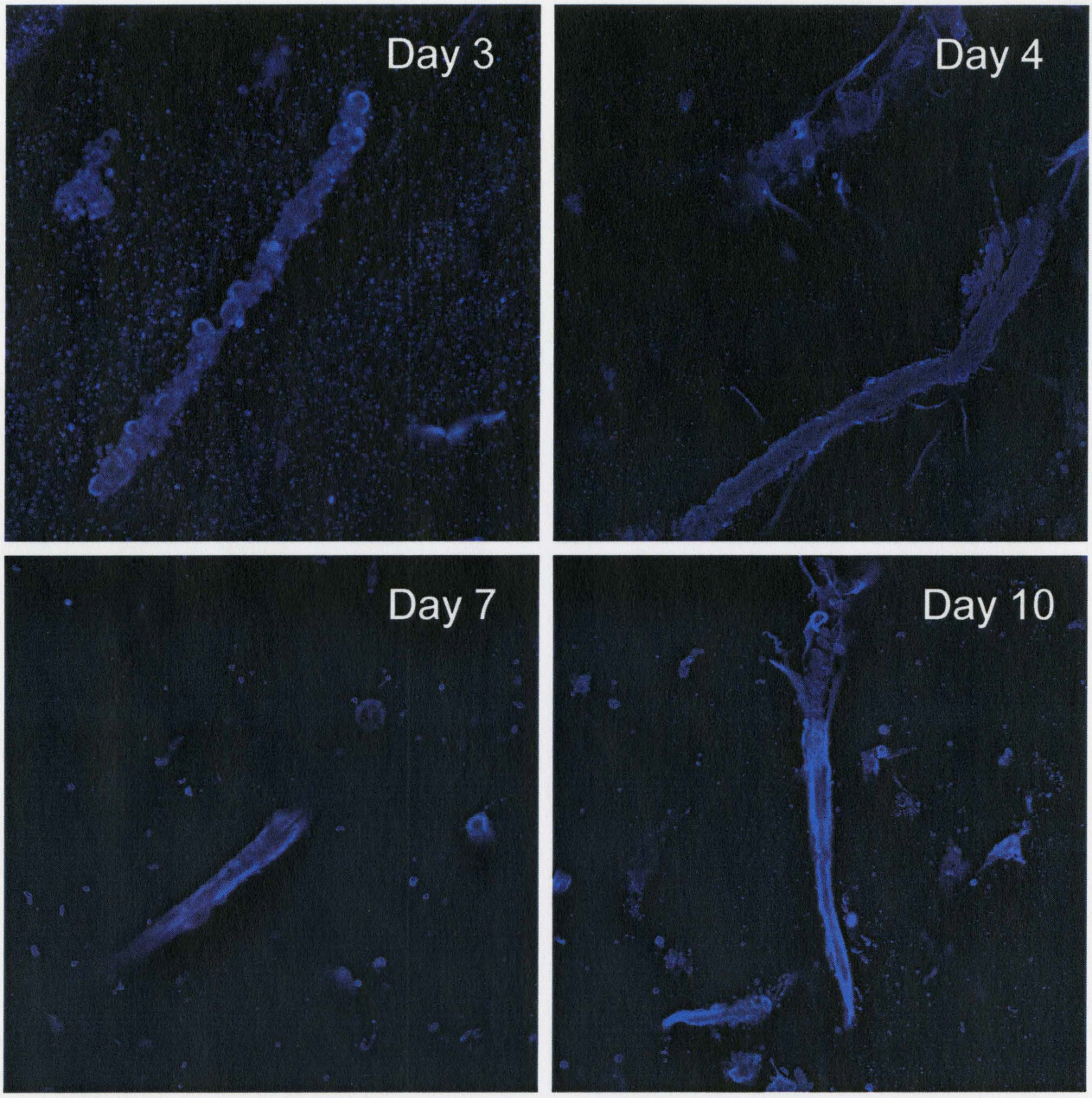

Figure 20. MMP-14 staining patterns of constructs at different times in the sprouting process. MMP-14 staining appears to becomes more and more prominent as the sprout grows in size.

Future Directions

At first, we though it would be most prudent to stain for MMPs during three distinct times of the sprouting process, day 4, day 7 and day 10 corresponding to early, mid and late sprouting of the microvessel fragments. This was based on the belief that MMP-2 and MMP-9 would show different staining patterns based on preliminary DNA microarray data obtained by the Hoying lab (unpublished data). Staining of these constructs did show some differences that were consistent with this data and needs to be explored to a greater extent. Staining of constructs at time points continuous with sprout growth would be beneficial and should help to solidify the observations which are made by the data shown in this report. These experiments were planned but lack of constructs prevented them from being performed. Since antibody staining cannot be adequately quantified, it might prove useful to perform quantitative real-time PCR and/or western blot analysis along these same time points to support the findings of antibody staining. Additionally, improvements could be made in the fixing and staining process which might mitigate the problems associated with the day 10 constructs.

MMP: Localization of Activity

Background

After determining the presence of MMP-2, MMP-9 and MMP-14 in the microvessel constructs, it will be necessary to show enzyme activity in order to prove that the enzymes are not merely present, but active to help bolster our knowledge of the involvement of each enzyme during angiogenesis within the context of our model system. Traditional methods for detecting MMP activity such as gelatin zymography or

fluorometric assays have been used successfully yet such methods do not help to localize the activity as a sample must be homogenized or otherwise destroyed. We would like to image the activity of MMPs within intact microvessel constructs so that we can show where along the vessels each enzyme is active and during which time points each is most or least active. We have envisioned a novel approach using fluorogenic substrates which would enable us to use advanced imaging processes to visualize the activity of each enzyme of interest.

Localization of MMP activity using fluorogenic substrates. Imaging of antibody staining of microvessel constructs is the first step to understanding the role an enzyme might play during angiogenesis. In order to confirm that an enzyme is involved in the process, it is not nearly adequate to simply show the presence of said enzyme. It becomes necessary to show that the enzyme is not only present, but active. Assays that show enzyme activity in biological samples has been done for years and is instructive, but limited due to the destructive nature of the testing. Fluorogenic substrates (Calbiochem, San Diego, CA) have been around for over two decades and have been used to assay for enzyme activity using standard spectroscopy which requires the homogenization of the sample of interest and sufficient purification. These substrates are relatively specific and are in the ultraviolet (UV) region of the light spectrum typically with excitation around 270-320nm which is out of the range of most visible lasers. Recently, fluorogenic assays have been developed for the MMPs of interest using fluorescence resonance energy transfer (FRET) engineered substrates which allow for excitation ranges between 450-520nm (AnaSpec, San Jose, CA). These excitation ranges are easily attainable by standard lasers but one

major problem exists in using these substrates, specificity. FRET substrates typically interact with multiple MMPs which limits a researcher's ability to show specific activity of an enzyme of interest (**Table 2**).

Product Name	Excitation	Emission	Reactivity
Enzolyte 520 MMP-14 Assay Kit	490nm ± 20nm	520nm ± 20nm	MMP-1,2,7,8,12,13,14
SensoLyte Plus 520 MMP-9 Assay Kit	490nm ± 20nm	520nm ± 20nm	MMP-9
SensoLyte 520 MMP-2 Assay Kit	490nm ± 20nm	520nm ± 20nm	MMP-1,8,9,12,13,14

Table 2

General protease activity can be obtained using products such as DQ gelatin (Invitrogen, Carlsbad, CA) but again are even less specific. We have envisioned two potential approaches to address the problem at hand. One of the methods is to use FRET substrates in conjunction with real-time PCR to show which of the MMPs outlined in the product sheet is contributing the most to the signal observed by single photon fluorescence excitation. This method would help to identify the main contributor of fluorescence signal but might not prove fruitful if an MMP that does not interest us is the major contributor. One might also consider experiments where the other MMPs are inhibited by either antibody blockade or inhibition by one of the tissue inhibitors of matrix metalloproteinases (TIMP).

A second, more theoretical approach is to use multiphoton excited fluorescence. Two photon excitation has been widely studied and used in recent years, however, due to the nature of the excitation ranges of these substrates, a standard two photon laser operating in the 700-1000nm range will not be capable of exciting them. In theory, three photon excited fluorescence will excite in the desired range. Three photon excited fluorescence (3PEF) has been described in the literature starting in the mid 1990 [83, 84]. We reasoned that three photon excitation could be used to activate fluorogenic substrates actively

excited in the UV range of interest by tuning the laser between 840nm and 960nm thereby giving us an effective range of three photon excitation of 280-320nm which nicely fits the range of specific fluorogenic substrates commercially available. Since nobody has described three photon fluorescence in these fluorogenic substrates and the fact that there are no three photon controls commercially available, we devised a strategy to test that the laser system would be able to produce three photon activity and detect it. We used rat tails which are rich in collagen as the test subject. The thought was that collagen crosslinking would somehow show up in the three photon range. Preliminary results showed that we could see very little 3PEF in the rat tail collagen until we used higher laser power and with increased exposure time. This produced some sort of optical effect that increased with time exposed to the laser. We filtered under 400nm and did see something which we concluded had to be 3PEF, though we believed this to be an artifact caused by prolonged laser exposure (**Figure 21**).

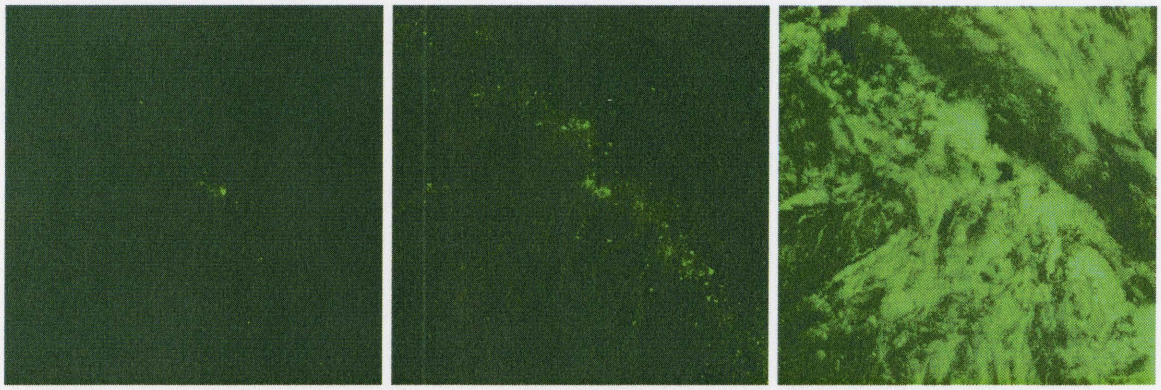

Figure 21. 840nm Excitation, filtered below 400nm. Left to right, 40% laser power, 60%, and 100%. Elapsed time: approximately 20 minutes.

Future Directions

The next step is to develop a strategy for testing the capability of the fluorogenic substrates to produce 3PEF. This is problematic because the manufacturers have no positive controls available as the substrates are synthesized in the quenched position and

only cleavage by the respective MMPs will activate the molecules. The strategy that might be best is to mix the substrate with purified and activated MMP enzyme then use multiphoton excitation to test for 3PEF. Once it has been verified that 3PEF is attainable using fluorogenic substrates, application of the substrates to living microvessel constructs is the next step. One approach is to apply the substrates to the constructs approximately 24 hours prior to imaging to allow for enough substrate to be cleaved. This time period is purely speculative but serves as a basis from which to start. The constructs would then be imaged using multiphoton microscopy. There are several potential problems associated with this approach including contamination of the fluorescence signal by culture media, excessive moving of the construct could displace cleaved enzyme, destruction of the sample from prolonged exposure to laser etc. Initial results will help clarify problem points in the process.

Appendix

Glycation crosslinking protocol

Making collagen gels: 2mL final volume required for this experiment.

1. Need 3mg/mL collagen therefore need to normalize from a more concentrated solution

$$\frac{3mg/mL}{4.32mg/mL} x 2.0mL = 1.327mL$$

2. 1x Hanks medium (starting conc. 10x) therefore need 200µL

3. 20mM HEPES therefore need 40µL HEPES

4. Add sterile H_2O to 2mL
   1.327mL collagen
   .2mL Hanks
   .04mL HEPES
   .433mL H_2O

5. pH to ~7.4 using 1M NaOH

8 gels loaded into a 48 well plate (~200µL per gel)

6. Incubate gels at 37C for 30 minutes or until set

7. Place media on gels, 4 concentration of glucose were used along with m199 reagent

8. No glu added in first two wells (5mM glu standard with m199 reagent)

9. 15mM glu in m199 added to 3rd and 4th wells
   Glu FW = 180.16g/mole
   .15mM solution = 180.16g/mole x 1mole/1000mL = .18016g/mL x .015 = .0027 or 2.7mg/mL etc (30mM and 50mM concentrations calculated similarly)

10. 30mM glu in m199 added to 5th and 6th wells

11. 50mM glu in m199 added to 7th and 8th wells

Gels incubated for 4 weeks at ~4C

En bloc immunostaining protocol

1. Remove microvessel fragment gels from well plates and place in micrfuge tube.
2. Wash briefly in 1x PBS.
3. Fix by incubating gels in 2% paraformaldehyde in 1x PBS for 15 minutes.
4. Place gels in fresh PBS until ready to use.
5. Incubate constructs in .25% triton X100 in DCF-PBS for 10 minutes.
6. Wash in DCF-PBS for 5 minutes.
7. Add 3 drops of Image II signal reducer and incubate for 30 minutes.
8. Remove Image II signal reducer and add 100μL 10% goat serum and incubate for 30 minutes.
9. Mouse IgG_3 anti-MMP-14 monoclonal antibody (Chemicon, Temecula, CA) was added at a 1:500 concentration in DCF-PBS and incubated for 2 hours.
10. Wash in DCF-PBS 2x for 5 minutes and 1x for 60 minutes.
11. Goat anti-mouse IgG_3 tagged with Alexa Fluor 488 (Molecular Probes, Eugene, OR) was added at a 1:500 concentration in DCF-PBS and incubated for 1 hour then washed in DCF-PBS 2x for 5 minutes and 1x for 60 minutes.

Zenon Mouse IgG labeling kit (Molecular Probes, Eugene, OR) was used for staining with MMP-2 and MMP-9

12. Add 1μL anti mouse IgG_1 MMP-2 monoclonal antibody (Chemicon, Temecula, CA) to 5μL Alexa Fluor 555 (Molecular Probes, Eugene, OR).
13. Add 3.2μL anti mouse IgG_1 MMP-9 monoclonal antibody (Chemicon, Temecula, CA) to 5μL Alexa Fluor 647 (Molecular Probes, Eugene, OR).
14. Incubate both for 5 minutes.
15. Add 5μL Zenon blocking reagent (Molecular Probes, Eugene, OR) to both and incubate for 5 minutes.
16. Add each mixture to 500μL DCF-PBS. Use 250μL of each per construct.
17. Incubate overnight. Wash in DCF-PBS 2x for 5 minutes and 1x for 60 minutes.

Transglutaminase crosslinking protocol

Obtain transglutaminase from n-zyme inc

Making collagen gels: 1mL final volume required for this experiment.

1. Need 3mg/mL collagen therefore need to normalize from a more concentrated solution

$$\frac{3mg/mL}{4.32mg/mL} x1.0mL = .694mL$$

2. 1x Hanks medium (starting conc. 10x) therefore need 100µL

3. 20mM HEPES therefore need 20µL HEPES

4. Add sterile H_2O to 2mL
   .694mL collagen
   .1mL Hanks
   .02mL HEPES
   .217mL H_2O

5. pH to ~7.4 using 1M NaOH

6. aliquot the gels into 2 sets of 400µL each

7. 2 vials add nothing

8. 2 vials add 5000:1 transglutaminase to collagen

9. load into a 48 well plate (~200µL per gel)

10. Incubate gels at 37C for 30 minutes or until set

11. Image gels

Rat Fat Microfragment (RFMF) Isolation Protocol

Required Supplies	
Solutions (sterile)	instruments (sterilized)
[ ] - *250mL* of 0.1% BSA in DCF-PBS (BSA-PBS) [ ] - *30mL* of BSA-PBS in 50mL tube [ ] - 2mg/mL Type 1 collagenase and 1mg/mL DNAse in BSA-PBS (col-DNAse-PBS) ***make 1.5x volume of collected fat calculations in step 2a* [ ] - type 1 rat tail collagen (greater than 3mg/mL) [ ] - 1M NaOH [ ] - sterile H_2O see recipes @ end: [ ] - 4x DMEM (less than 1 week old) [ ] - RFMF media (make fresh each time)	[ ] - surgical pack: 4" gauze (*x2 per rat*), 1 large scissors, 1 small scissors, 1 hemostat, 1 forceps [ ] - mincing pack: 1 curved scissors, 1 forceps [ ] - metal rack to support 30μm screen [ ] - 50mL polycarbonate flasks w/ stir-bar (*x1 per 6mL collected fat*) [ ] - 2 screens (30μm and 500μm) [ ] - 100mm x 20mm petri dishes *x4* (NOT TISSUE CULTURE TREATED) [ ] - 50mL centrifuge tubes *x3* [ ] - 15mL centrifuge tubes *x3* [ ] - 10mL syringe [ ] - 0.2μm syringe filter (*1x 15mL col-DNAse-PBS*) [ ] - 48 well plate [ ] - sterile 10mL pipettes

1. Surgery (need surgical pack, 30mL of BSA-PBS in 50mL tube)

a. Anesthetize animal with Isofluorane, then inject inter-peritoneal with 1.5mL Nembutol (see illustration 1).

b. Once animal is anesthetized, spray abdomen with Nolvasan.

c. Clamp skin, just below penis, with hemostat. Begin incision with large scissors, starting in the center and cutting laterally (see illustration 1).

d. Place 2 folded sterile gauze pads below incision (see illustration 2).

e. With small scissors, make a small incision into each scrotum, exposing the epidydimal fat.

f. With forceps, carefully remove the testes and epidydimal fat pads from the animal and place on sterile gauze. (illustration 2)

g. With forceps, pull the fat from the testes and cut using the small scissors.

h. Carefully place removed fat into 50mL tube with BSA-PBS. Final volume of fat + BSA-PBS - 30mL = *fat volume*

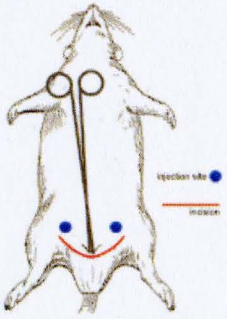

illustration 1

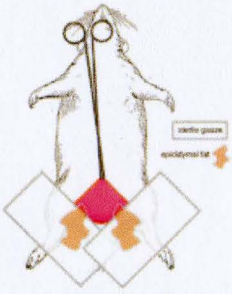

illustration 2

2. RFMF isolation (need BSA-PBS, mincing pack, water bath set to 37°C, metal rack, 30μm and 500μm screens, flasks w/ stir-bars, petri-dishes, 50mL and 15mL centrifuge tubes, 48 well plate, syringe and syringe filter, sterile 10mL pipettes)

a. Measure collagenase and DNAse. **NOTE: combine collagenase and DNAse in same 50mL tube, keep in freezer until use**
   collagenase (mg) = *fat volume x 3*
   DNAse (mg) = *fat volume x 1.5*
   BSA-PBS (mL) = *fat volume x 1.5* **NOTE: do not add BSA-PBS until step c**

b. Place all the fat in a petri dish. Mince with curved scissors for 10 minutes. When finished, fat should not clog tip of 10mL pipette.

c. Mix *step a* components (col-DNAse-PBS) in 50mL tube, sterilize with syringe filter into petri dish. Mix gently with scissors.

d. Divide rat fat-col-DNAse-PBS evenly into 50mL polycarbonate flasks. Agitate briskly for 6 min in 37°C water bath. When finished, there should be only a few small fat particulates visible w/in the flask.

e. Divide rat fat-col-DNAse-PBS evenly into two 50mL centrifuge tubes (if small volume, 15mL tubes may be used instead). Centrifuge at 400rcf for 4 minutes.

f. Carefully decant (or pipette if preferred) supernatant and adipocytes (be sure to not disturb pellet at bottom of tube).

g. Add 10mL of BSA-PBS to each tube. Gently titrate against side of tube to break up pellet 4x. Transfer everything evenly to two 15mL tubes. Centrifuge at 400rcf for 4 minutes.

h. Repeat f and g 2x

i. During last spin, presoak 30μm screen in ~20mL BSA-PBS within a covered petri dish. With sterile forceps, place 500μm screen above petri dish and presoak with ~5mL BSA-PBS pipetted on top of screen.

j. Aspirate fragment suspension a few times and then slowly pipette over 500μm screen. Move outward from center in concentric circles. When finished, rinse tube with ~5mL BSA-PBS and pipette over screen in similar manner. Discard 500μm screen.

k. With sterile forceps, place wire mesh on top of petri dish. Then center 30μm screen on wire mesh.
   Pipette filtered fragment suspension over 30μm screen in concentric circles. Take care to prevent
   suspension from spilling over the sides of the screen.

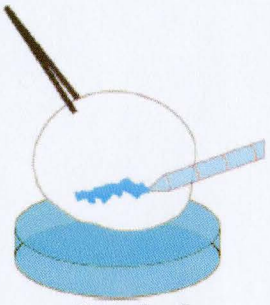
illustration 3

l. Rinse the screen gently with 5mL BSA-PBS.

m. With sterile forceps, slide 30μm screen from wire mesh into petri dish with 20mL BSA-PBS. Gently shake petri dish to dislodge fragments from the screen.

n. Place the back of the petri dish on the lid (angling the dish forward). With forceps, grab the top of the screen and slowly raise from the petri dish. Simultaneously, use 10mL of BSA-PBS and rinse the screen with a back-and-forth motion. (see illustration 3)

o. Collect the filtered fragment-BSA-PBS suspension and dispense into a 50mL tube.

p. To count fragments, clip ~20% off the end of a 200μL pipette tip. Gently shake the 50mL tube containing the fragment-BSA-PBS suspension. Remove two 20μL samples of suspension and dispense on a glass slide or petri dish lid. Under a microscope, count the fragments:
Total Fragments = (ave fragment count) * (total mL suspension in 50mL tube) * 50

q. Centrifuge fragment-BSA-PBS suspension at 400rcf for 4 minutes. Carefully decant or aspirate the supernatant. Leave ~200μL above the pellet.

3. Suspend RFMFs in collagen (need 48 well plate, 4x DMEM, 1M NaOH, Sterile H_20, Type 1 Rat Tail Collagen, bucket of ice, RFMF Media)

a. Place 4x DMEM, 1M NaOH, Sterile H_20, Type 1 Rat Tail Collagen, and a 15mL tube into ice bucket.

b. Determine total collagen suspension volume required for [RFMF] of 15,000 - 20,000 RFMF / mL. Add an extra 0.5 to 1mL to compensate for tube and pipette wall adhesion. Final [collagen] is 3mg/mL.
i. Determine volume of collagen required to yield 3mg/mL
ii. Determine volume of 4x DMEM = collagen volume / 3
iii. Determine volume of water = (final total volume) - (collagen volume) - (4x DMEM volume)
iv. Add SMALL volumes 1M NaOH until appropriate suspension pH (mixture color) is reached

c. Gently flick 50mL tube to break up RFMF pellet. Slowly dispense collagen suspension. Take care to avoid introducing bubbles. Pipette until fragments are fully suspended. Add additional NaOH if required.

d. Pipette fragment-collagen suspension into 48-well plates. Add 250μL per well.

e. Place well plate in sterile incubator (37°C, 5% CO_2) for 20 minutes.

f. Add 250μL of RFMF media to each well. Place well plate back into incubator.

g. Change media every 4 days. Fragments should show appreciable sprouting by day 4.

Media Recipes

RFMF media:
9mL 1x DMEM media (VWR 10-014-CV, invitrogen 11885-084)
1mL heat inactivated Fetal Bovine Serum

**make fresh and filter sterilize before each use

4x DMEM:
1g GIBCO DMEM powder (invitrogen 31600-034 or 026)
0.37g $NaHCO_3$
0.476g HEPES (sigma H7006)
add Sterile H_2O to bring volume up to 25mL

**filter sterilize before use
**make new 4x DMEM every 7 days

References

1. Fisher, C., et al., *Interstitial collagenase is required for angiogenesis in vitro.* Dev Biol, 1994. **162**(2): p. 499-510.
2. Haas, T.L., S.J. Davis, and J.A. Madri, *Three-dimensional type I collagen lattices induce coordinate expression of matrix metalloproteinases MT1-MMP and MMP-2 in microvascular endothelial cells.* J Biol Chem, 1998. **273**(6): p. 3604-10.
3. Jain, A., et al., *Production of cytokines, vascular endothelial growth factor, matrix metalloproteinases, and tissue inhibitor of metalloproteinases 1 by tenosynovium demonstrates its potential for tendon destruction in rheumatoid arthritis.* Arthritis Rheum, 2001. **44**(8): p. 1754-60.
4. Risau, W., *Mechanisms of angiogenesis.* Nature, 1997. **386**(6626): p. 671-4.
5. Vernon, R.B. and E.H. Sage, *A novel, quantitative model for study of endothelial cell migration and sprout formation within three-dimensional collagen matrices.* Microvasc Res, 1999. **57**(2): p. 118-33.
6. Ausprunk, D.H. and J. Folkman, *Migration and proliferation of endothelial cells in preformed and newly formed blood vessels during tumor angiogenesis.* Microvasc Res, 1977. **14**(1): p. 53-65.
7. Adams, R.H., et al., *Roles of ephrinB ligands and EphB receptors in cardiovascular development: demarcation of arterial/venous domains, vascular morphogenesis, and sprouting angiogenesis.* Genes Dev, 1999. **13**(3): p. 295-306.
8. Breier, G., *Angiogenesis in embryonic development--a review.* Placenta, 2000. **21 Suppl A**: p. S11-5.
9. Holmgren, L., et al., *Angiogenesis during human extraembryonic development involves the spatiotemporal control of PDGF ligand and receptor gene expression.* Development, 1991. **113**(3): p. 749-54.
10. Battegay, E.J., *Angiogenesis: mechanistic insights, neovascular diseases, and therapeutic prospects.* J Mol Med, 1995. **73**(7): p. 333-46.
11. Bray, R.C., R.M. Rangayyan, and C.B. Frank, *Normal and healing ligament vascularity: a quantitative histological assessment in the adult rabbit medial collateral ligament.* J Anat, 1996. **188 (Pt 1)**: p. 87-95.
12. Bray, R.C., et al., *Vascular response of the meniscus to injury: effects of immobilization.* J Orthop Res, 2001. **19**(3): p. 384-90.
13. Ravanti, L. and V.M. Kahari, *Matrix metalloproteinases in wound repair (review).* Int J Mol Med, 2000. **6**(4): p. 391-407.
14. Blavier, L., et al., *Tissue inhibitors of matrix metalloproteinases in cancer.* Ann N Y Acad Sci, 1999. **878**: p. 108-19.
15. Folkman, J., *Angiogenesis in cancer, vascular, rheumatoid and other disease.* Nat Med, 1995. **1**(1): p. 27-31.
16. Grant, D.S., et al., *Decorin suppresses tumor cell-mediated angiogenesis.* Oncogene, 2002. **21**(31): p. 4765-77.
17. Valente, P., et al., *TIMP-2 over-expression reduces invasion and angiogenesis and protects B16F10 melanoma cells from apoptosis.* Int J Cancer, 1998. **75**(2): p. 246-53.

18. Vergani, V., et al., *Inhibition of matrix metalloproteinases by over-expression of tissue inhibitor of metalloproteinase-2 inhibits the growth of experimental hemangiomas.* Int J Cancer, 2001. **91**(2): p. 241-7.
19. Henriet, P., L. Blavier, and Y.A. Declerck, *Tissue inhibitors of metalloproteinases (TIMP) in invasion and proliferation.* Apmis, 1999. **107**(1): p. 111-9.
20. Rivilis, I., et al., *Differential involvement of MMP-2 and VEGF during muscle stretch- versus shear stress-induced angiogenesis.* Am J Physiol Heart Circ Physiol, 2002. **283**(4): p. H1430-8.
21. Tranqui, L. and P. Tracqui, *Mechanical signalling and angiogenesis. The integration of cell-extracellular matrix couplings.* C R Acad Sci III, 2000. **323**(1): p. 31-47.
22. Vailhe, B., et al., *In vitro angiogenesis is modulated by the mechanical properties of fibrin gels and is related to alpha(v)beta3 integrin localization.* In Vitro Cell Dev Biol Anim, 1997. **33**(10): p. 763-73.
23. Vernon, R.B. and E.H. Sage, *Contraction of fibrillar type I collagen by endothelial cells: a study in vitro.* J Cell Biochem, 1996. **60**(2): p. 185-97.
24. Hoying, J.B., C.A. Boswell, and S.K. Williams, *Angiogenic potential of microvessel fragments established in three-dimensional collagen gels.* In Vitro Cell Dev Biol Anim, 1996. **32**(7): p. 409-19.
25. Kirkpatrick, N.D., et al., *Live imaging of collagen remodeling during angiogenesis.* Am J Physiol Heart Circ Physiol, 2007. **292**(6): p. H3198-206.
26. Krishnam L, H.J., Das R, Weiss JA. *Alterations in the material properties of collagen by angiogenesis*. in *Proc 49th Annual Orthopaedic Research Society Meeting*. 2003.
27. Krishnan L, H.J., Nguyen H, Song H, Weiss JA, *Interaction of angiogenic microvessels with the extracellular matrix in an in vitro model.* American Journal of Physiology: Heart and Circulation, 2007. **In review**.
28. Shepherd, B.R., et al., *Rapid perfusion and network remodeling in a microvascular construct after implantation.* Arterioscler Thromb Vasc Biol, 2004. **24**(5): p. 898-904.
29. Bergers, G. and S. Song, *The role of pericytes in blood-vessel formation and maintenance.* Neuro Oncol, 2005. **7**(4): p. 452-64.
30. Egginton, S., et al., *The role of pericytes in controlling angiogenesis in vivo.* Adv Exp Med Biol, 2000. **476**: p. 81-99.
31. Lafleur, M.A., et al., *Perivascular cells regulate endothelial membrane type-1 matrix metalloproteinase activity.* Biochem Biophys Res Commun, 2001. **282**(2): p. 463-73.
32. Ozerdem, U. and W.B. Stallcup, *Early contribution of pericytes to angiogenic sprouting and tube formation.* Angiogenesis, 2003. **6**(3): p. 241-9.
33. Redmer, D.A., et al., *Evidence for a role of capillary pericytes in vascular growth of the developing ovine corpus luteum.* Biol Reprod, 2001. **65**(3): p. 879-89.
34. Saito, M., et al., *Single-column high-performance liquid chromatographic-fluorescence detection of immature, mature, and senescent cross-links of collagen.* Anal Biochem, 1997. **253**(1): p. 26-32.
35. Greenwald, S.E. and C.L. Berry, *Improving vascular grafts: the importance of mechanical and haemodynamic properties.* J Pathol, 2000. **190**(3): p. 292-9.

36. Hirai, J. and T. Matsuda, *Self-organized, tubular hybrid vascular tissue composed of vascular cells and collagen for low-pressure-loaded venous system.* Cell Transplant, 1995. **4**(6): p. 597-608.
37. L'Heureux, N., et al., *In vitro construction of a human blood vessel from cultured vascular cells: a morphologic study.* J Vasc Surg, 1993. **17**(3): p. 499-509.
38. Weinberg, C.B. and E. Bell, *A blood vessel model constructed from collagen and cultured vascular cells.* Science, 1986. **231**(4736): p. 397-400.
39. Balgude, A.P., et al., *Agarose gel stiffness determines rate of DRG neurite extension in 3D cultures.* Biomaterials, 2001. **22**(10): p. 1077-84.
40. Bell, E., et al., *Living tissue formed in vitro and accepted as skin-equivalent tissue of full thickness.* Science, 1981. **211**(4486): p. 1052-4.
41. Lafrance, H., et al., *Study of the tensile properties of living skin equivalents.* Biomed Mater Eng, 1995. **5**(4): p. 195-208.
42. Michel, M., F.A. Auger, and L. Germain, *Anchored skin equivalent cultured in vitro: a new tool for percutaneous absorption studies.* In Vitro Cell Dev Biol Anim, 1993. **29A**(11): p. 834-7.
43. Wilkins LM, W.S., Prosky SJ, Meunier SF, Parenteau NL, *Development of a bilayered skin construct for clinical applications.* Biotechnol Bioeng, 1994. **43**: p. 747-56.
44. Mauck, R.L., et al., *Functional tissue engineering of articular cartilage through dynamic loading of chondrocyte-seeded agarose gels.* J Biomech Eng, 2000. **122**(3): p. 252-60.
45. Toolan, B.C., et al., *Effects of growth-factor-enhanced culture on a chondrocyte-collagen implant for cartilage repair.* J Biomed Mater Res, 1996. **31**(2): p. 273-80.
46. Porter, B.D., et al., *Mechanical properties of a biodegradable bone regeneration scaffold.* J Biomech Eng, 2000. **122**(3): p. 286-8.
47. Huang, D., et al., *Mechanisms and dynamics of mechanical strengthening in ligament-equivalent fibroblast-populated collagen matrices.* Ann Biomed Eng, 1993. **21**(3): p. 289-305.
48. Koide, T. and M. Daito, *Effects of various collagen crosslinking techniques on mechanical properties of collagen film.* Dent Mater J, 1997. **16**(1): p. 1-9.
49. Suh, H., et al., *A bone replaceable artificial bone substitute: cytotoxicity, cell adhesion, proliferation, and alkaline phosphatase activity.* Artif Organs, 2001. **25**(1): p. 14-21.
50. Weadock, K.S., et al., *Physical crosslinking of collagen fibers: comparison of ultraviolet irradiation and dehydrothermal treatment.* J Biomed Mater Res, 1995. **29**(11): p. 1373-9.
51. Goissis, G., et al., *The chemical protecting group concept applied in crosslinking of natural tissues with glutaraldehyde acetals.* Artif Organs, 1998. **22**(3): p. 210-4.
52. Jayakrishnan, A. and S.R. Jameela, *Glutaraldehyde as a fixative in bioprostheses and drug delivery matrices.* Biomaterials, 1996. **17**(5): p. 471-84.
53. Kanamori T, H.T., Shinbo T, Sakai K, *Difference in solute diffusivity in crosslinked collagen gels prepared under various conditions.* Mater Sci Eng C, 2000. **13**: p. 85-9.

54. Olde Damink LLH, D.P., van Luyn MJ, van Wachem PB, Nieuwenhuis P, Feijen J, *Glutaraldehyde as a crosslinking agent for collagen based biomaterials.* J Mater Sci Mater Med, 1995. **6**: p. 460-72.
55. Chevallay, B., N. Abdul-Malak, and D. Herbage, *Mouse fibroblasts in long-term culture within collagen three-dimensional scaffolds: influence of crosslinking with diphenylphosphorylazide on matrix reorganization, growth, and biosynthetic and proteolytic activities.* J Biomed Mater Res, 2000. **49**(4): p. 448-59.
56. Bellincampi LD, D.M., *Effect of crosslinking method on collagen fiber–fibroblast interactions.* .J Appl Polym Sci, 1998. **63**: p. 1423-28.
57. Girton, T.S., T.R. Oegema, and R.T. Tranquillo, *Exploiting glycation to stiffen and strengthen tissue equivalents for tissue engineering.* J Biomed Mater Res, 1999. **46**(1): p. 87-92.
58. Noishiki, Y., et al., *Succinylated collagen crosslinked by thermal treatment for coating vascular prostheses.* Artif Organs, 1998. **22**(8): p. 672-80.
59. Pieper, J.S., et al., *Attachment of glycosaminoglycans to collagenous matrices modulates the tissue response in rats.* Biomaterials, 2000. **21**(16): p. 1689-99.
60. Rault I, F.V., Herbage D, Abdul-Malak N, Huc A, *Evaluation of different chemical methods for crosslinking collagen gels, films, and sponges.* J Mater Sci Mater Med, 1996. **7**: p. 215-22.
61. Simmons, D.M. and J.N. Kearney, *Evaluation of collagen cross-linking techniques for the stabilization of tissue matrices.* Biotechnol Appl Biochem, 1993. **17 (Pt 1)**: p. 23-9.
62. Wissink, M.J., et al., *Endothelial cell seeding on crosslinked collagen: effects of crosslinking on endothelial cell proliferation and functional parameters.* Thromb Haemost, 2000. **84**(2): p. 325-31.
63. Aeschlimann, D. and M. Paulsson, *Transglutaminases: protein cross-linking enzymes in tissues and body fluids.* Thromb Haemost, 1994. **71**(4): p. 402-15.
64. Orban, J.M., et al., *Crosslinking of collagen gels by transglutaminase.* J Biomed Mater Res A, 2004. **68**(4): p. 756-62.
65. Elbjeirami, W.M., et al., *Enhancing mechanical properties of tissue-engineered constructs via lysyl oxidase crosslinking activity.* J Biomed Mater Res A, 2003. **66**(3): p. 513-21.
66. Lau, Y.K., A.M. Gobin, and J.L. West, *Overexpression of lysyl oxidase to increase matrix crosslinking and improve tissue strength in dermal wound healing.* Ann Biomed Eng, 2006. **34**(8): p. 1239-46.
67. Speer, D.P., et al., *Biological effects of residual glutaraldehyde in glutaraldehyde-tanned collagen biomaterials.* J Biomed Mater Res, 1980. **14**(6): p. 753-64.
68. Egeblad, M. and Z. Werb, *New functions for the matrix metalloproteinases in cancer progression.* Nat Rev Cancer, 2002. **2**(3): p. 161-74.
69. Chakraborti, S., et al., *Regulation of matrix metalloproteinases: an overview.* Mol Cell Biochem, 2003. **253**(1-2): p. 269-85.
70. Arvelo, F. and C. Cotte, *[Metalloproteinases in tumor progression. Review].* Invest Clin, 2006. **47**(2): p. 185-205.
71. Deryugina, E.I. and J.P. Quigley, *Matrix metalloproteinases and tumor metastasis.* Cancer Metastasis Rev, 2006. **25**(1): p. 9-34.

72. Fingleton, B., *Matrix metalloproteinases: roles in cancer and metastasis.* Front Biosci, 2006. **11**: p. 479-91.
73. Golubkov, V.S. and A.Y. Strongin, *Proteolysis-driven oncogenesis.* Cell Cycle, 2007. **6**(2): p. 147-50.
74. Malemud, C.J., *Matrix metalloproteinases (MMPs) in health and disease: an overview.* Front Biosci, 2006. **11**: p. 1696-701.
75. Rosenthal, E.L. and L.M. Matrisian, *Matrix metalloproteases in head and neck cancer.* Head Neck, 2006. **28**(7): p. 639-48.
76. Hanahan, D. and R.A. Weinberg, *The hallmarks of cancer.* Cell, 2000. **100**(1): p. 57-70.
77. Chun, T.H., et al., *MT1-MMP-dependent neovessel formation within the confines of the three-dimensional extracellular matrix.* J Cell Biol, 2004. **167**(4): p. 757-67.
78. Masson, V., et al., *Contribution of host MMP-2 and MMP-9 to promote tumor vascularization and invasion of malignant keratinocytes.* Faseb J, 2005. **19**(2): p. 234-6.
79. Masson V Ve, D.L., Grignet-Debrus C, Bernt S, Bajou K, Blacher S, Roland G, Chang Y, Fong T, Carmeliet P, Foidart JM, Noel A. .*Mouse Aortic Ring Assay: A New Approach of the Molecular Genetics of Angiogenesis.* in *Biol Proced Online.* 2002.
80. Yue, P.Y., et al., *The angiosuppressive effects of 20(R)- ginsenoside Rg3.* Biochem Pharmacol, 2006. **72**(4): p. 437-45.
81. Ghajar, C.M., et al., *Mesenchymal stem cells enhance angiogenesis in mechanically viable prevascularized tissues via early matrix metalloproteinase upregulation.* Tissue Eng, 2006. **12**(10): p. 2875-88.
82. Genis, L., et al., *MT1-MMP: universal or particular player in angiogenesis?* Cancer Metastasis Rev, 2006. **25**(1): p. 77-86.
83. Szmacinski, H., I. Gryczynski, and J.R. Lakowicz, *Three-photon induced fluorescence of the calcium probe Indo-1.* Biophys J, 1996. **70**(1): p. 547-55.
84. Lakowicz, J.R., *Emerging applications of fluorescence spectroscopy to cellular imaging: lifetime imaging, metal-ligand probes, multi-photon excitation and light quenching.* Scanning Microsc Suppl, 1996. **10**: p. 213-24.